scientific reports

OPEN

Unveiling spatiotemporal dynamics and drivers of ecosystem services to optimize the ecological zoning management in the Luo river basin

Jing Zhang[1], Xuning Qiao[1,2✉], Yongju Yang[1], Liang Liu[1], Jinchan Zheng[1], Yuru Chen[1] & Yulong Dai[1]

The comprehensive ecosystem service index (CESI) and ecosystem service bundles (ES bundles) were integrated, combined with the optimal parameter geographic detector and multi-scale geographically weighted regression to reveal the spatiotemporal differentiation and driving mechanism of ecosystem services (ESs) in Luo River Basin. The results show that the spatial distribution of ESs is low in the northeast and high in the southwest, similar to the distribution of forests. The average annual growth rates of water yield, carbon storage, and soil retention were 4.71%, 0.05%, and 8.97% respectively, and the spatial increase area accounted for more than 90%. Habitat quality decreased by an average of 0.31% per year, with 39.76% of the region declining. The upstream ecological benefits of CESI are better than those of the downstream, and ES bundles identify two high supply modes (B2, B3). Precipitation, normalized difference vegetation index, and slope are the dominant driving factors of ESs and CESI. Based on the heterogeneity of driving responses, a watershed zoning governance framework is proposed. Upstream vegetation structure needs to be optimized; the disorderly expansion of downstream cities should be curbed to provide a scientific basis for the next stage of the Grain for Green program and spatially differentiated governance.

Keywords Spatiotemporal differentiation, Trend analysis, Optimal Parameter Geographic Detector (OPGD), Multi-scale geographically weighted regression (MGWR), Luo River basin

Ecosystem services (ESs) are the key link in maintaining human well-being and continuously support social development through material supply and functional regulation[1]. With rapid urbanization and land use transformation, a series of ecological and environmental problems such as biodiversity loss, degradation of water quality and soil erosion have occurred, seriously weakening the original ecosystem service supply capacity[2,3]. Policies such as the "Outline of the Plan for Ecological Protection and High-Quality Development of the Yellow River Basin" and the "Opinions of the Central Committee of the Communist Party of China and the State Council on Accelerating the Advancement of the Construction of Ecological Civilization"[4,5] require strengthening regional comprehensive ecological environment construction, including rural environmental governance and protection of river basins such as the Yangtze River and the Yellow River. Quantifying the dynamic changes of ESs and analyzing the driving forces to build a scientific decision-making basis is an important part of assessing ecosystem health[6]. Existing studies have mostly focused on watershed and urban scales[7,8]. Regulating ESs play a key role in mitigating climate change, preventing soil erosion and flooding, and improving food security. For example, Hisano et al. emphasized that protecting intact forest ecosystems and promoting the functional diversity of forests can enhance their adaptability and resilience to climate change[9]. Bunel et al. quantitatively analyzed the effects of vegetation coverage on runoff and sediment output at different time scales. The results showed that vegetation significantly regulated runoff and erosion responses[10]. Bekri et al. systematically investigated and studied the spatial distribution characteristics, ecological status, and ESs mapping assessment and value quantification of water ecosystems, indicating that water ecosystems (rivers, lakes, and groundwater) maintain the ecological security of the basin through core service functions such as water purification and water conservation[11]. Wang et al. incorporated the natural input and ecosystem service output of cultivated land

[1]School of Surveying and Land Information Engineering, Henan Polytechnic University, Jiaozuo 454003, China. [2]Research Centre of Arable Land Protection and Urban-Rural High-Quality Development of Yellow River Basin, Henan Polytechnic University, Jiaozuo 454003, China. ✉email: qiaoxuning@126.com

into the evaluation framework of ecological efficiency of cultivated land use (ECLU), improving the ecological function of cultivated land while ensuring food security[12].

Long-term quantitative analysis can capture subtle changes in geospatial information trends and drive the application of ESs from scientific research to policy formulation. Previous studies are often limited to a static evaluation framework of two-period comparison[13], which makes it difficult to capture the nonlinear characteristics and hysteresis effects of ESs evolution. An et al. conducted a temporal analysis of the dynamics of soil conservation services in major watersheds around the world, which is of great value for understanding long-term trends related to ecosystem services[14]. Qu et al.[15] analyzed the long-term trend changes of ecosystem services in Anhui Province and created a framework and index to evaluate the trade-offs and synergies of ecosystem services using spatial overlay and autocorrelation. Wu and Fan first introduced the Comprehensive Ecosystem Services Index (CESI), which integrated multiple ecosystem services for comprehensive assessment but did not consider the specific shares and contribution levels of different ecosystem services[16,17]. Ecosystem service bundles (ES bundles) reveal service association patterns through spatiotemporal clustering, which are combinations of ecosystem services that occur repeatedly in time or space and are closely related to each other[18,19]. Some studies identify ecosystem service clusters and similar ESs combinations based on K-means clustering algorithm[20], Gaussian mixture model[21], and principal component analysis[22]. This study uses an unsupervised artificial neural network self-organizing map (SOM) method to generate low-dimensional, discrete maps to identify ES bundles with high fault tolerance and stability[23]. Combining CESI and SOM can break through the limitations of a single method. CESI provides quantitative support for ES bundles, and ES bundles can refine the internal structure of CESI, realize the transition from single numerical evaluation to in-depth analysis of structure and function, improve the comprehensiveness and scientificity of the evaluation framework, and provide an important perspective for understanding the inherent connection and complexity of ecosystem services.

Changes in ecosystem services are jointly influenced by natural elements and human activities. Quantifying the impact of drivers on ESs and analyzing their drivers will coordinate ecological protection and improve management strategies. The effects of single factors on ESs have been extensively studied in detail from various perspectives, including land use change[24], urban expansion[25], and climate change[26]. Various studies have demonstrated the complexity of factors influencing ESs, including natural elements such as vegetation and elevation, climatic variables such as precipitation and temperature, and socio-economic indicators reflecting human activities[27,28]. Sannigrahi et al.[29] further confirmed that climate factors are highly correlated with ESs changes. The spatial heterogeneity of ESs is driven by the multi-scale interaction of natural-social factors, and the spatial regression model can better reflect the spatial heterogeneity of the impact of driving factors on ecosystem service trends than the non-spatial model[30]. Li et al.[31] thorough analysis of the effect of ESs in the Qiantang River basin of China, considering both natural and socio-economic factors using a random forest model. Su et al.[32] employed geographically weighted regression (GWR) to illustrate the correlation between ESs values and the spatial response to urbanization, which exhibited non-stationary characteristics. He et al.[33] employed the Geodetector (GD) to investigate the driving factors of typical ESs and to calculate the multiple ESs landscape index in the Yangtze River Economic Belt. GD has the advantage of handling spatial differentiation drivers and detecting interactions among multiple factors[34,35]. Furthermore, by accounting for spatial scale differences in various explanatory variables, multi-scale geographically weighted regression (MGWR) models can be utilized to accurately evaluate the spatial distribution and variation of influencing factors. In order to improve the models' predictive abilities and precision and to offer reliable support for scientific decision-making in the region's development, we integrated the GD and MGWR models in this study to precisely analyze the influencing factors of ESs at the township scale in the Luo River basin.

Luo River is one of the important tributaries of the Yellow River and is crucial to the development of ecological civilization in the Yellow River Basin. Previous studies on watershed ESs have mostly focused on the changes in certain ecosystem services in specific years, without combining temporal and spatial dimensions to conduct long-term trend change analysis. This study expands the previous ES bundles framework, integrates CESI and ES bundles methods to analyze the spatiotemporal evolution characteristics of multi-service collaboration, and explains the spatial distribution characteristics of different ecological environments from a comprehensive perspective. The influence of topography, climate, and socioeconomic development on ESs was further explored to reveal the spatial heterogeneity of the key driving factors affecting ESs. The main objectives of this study are: (1) to analyze the long-term temporal variation trend of ESs; (2) to explore the spatial distribution of the combined changes among multiple ESs; and (3) to determine the main driving factors affecting ESs and CESI and their spatial heterogeneity, and to divide ecological functional zones based on their spatial distribution. The research results provide differentiated management and control plans for watershed ecological protection, which is conducive to promoting the comprehensive and coordinated development of various ecosystems and providing a strong scientific basis for the protection of township ecosystems in the Luo River Basin and the development of high-quality watersheds.

Materials and methods
Research area
The Luo River basin lies within the borders of Luoyang City in southeastern Shaanxi Province and the northwestern Henan Province, China (33°39′–34°53′ N, 109°43′–113°09′ E), ultimately draining into the Yellow River at Gongyi City (Fig. 1). The watershed spans 447 km in length, covering a total land area of 18,769 km². Overall, 45.2% of the area comprises soil and rocky mountains, 51.3% consists of loess hills, and 3.5% of the land is composed of alluvial plains. The altitude ranges from 57 to 2655 m, it is located in the transition zone between the second and third terraces of China's terrain. The climate type is continental monsoon, which is defined by warm, rainy summers, chilly, dry winters, and moderate spring and fall temperatures[36]. The basin is intersected
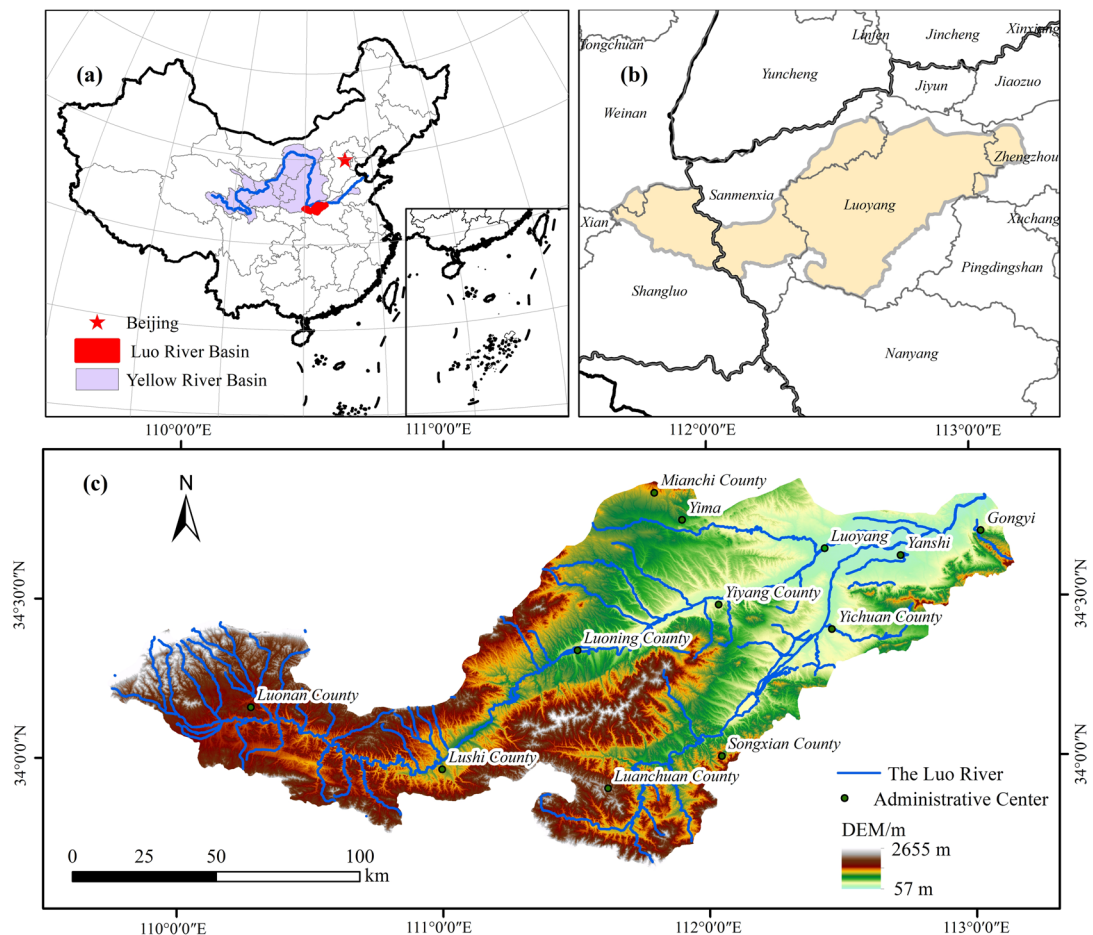
Fig. 1. (**a**) Geographic location, (**b**) land level location, and (**c**) elevation of the Luo River basin. Software version: ArcMap 10.8, URL: https://www.esri.com/zh-cn/arcgis/products/index. This map is produced based on the standard map with the review number GS(2024)0650, downloaded from the National Geographic Information Public Service Platform (website: https://www.tianditu.gov.cn/), and the base map has not been modified.

by numerous rivers, creating an intricate network of water systems. Tributaries play a crucial role in supporting local irrigation, agricultural production, and the domestic water supply. The Luo River basin, an essential part of the Yellow River basin, is the birthplace of Chinese civilization as well as a significant source of ecological resources. The ecological advantages offered by the basin are substantial. An undulating topography that features higher altitudes in the west and lower heights in the east has led to serious soil erosion in the middle reaches of the basin. With the advancement of the "Grain for Green" program (GFGP), the upstream forest area continues to expand, which is beneficial to the enhancement of the carbon storage capacity of ecosystem services and the protection of biodiversity. With the rapid economic development in the downstream areas, the habitat quality has seriously degraded, and over-exploitation of natural resources and environmental degradation in the Luo River Basin have occurred frequently.

Data sources

Numerous datasets were used in this investigation, including information on soil, topography, weather, land use, and socioeconomic conditions. The slope was calculated using ArcGIS software based on the Digital Elevation Model (DEM). The distance from the water system (WD) was calculated based on the Euclidean distance tool. The land use degree comprehensive index (LUDCI) was calculated based on the method described by Zhuang and Liu[37]. The geographic coordinate system of the data was defined as GCS_WGS_1984. The projected coordinate system was defined as WGS_1984_UTM_Zone_49N. Table 1 provides further details of the data and sources.

Quantitative methods and calculations

Overall Workflow

This study used Sen trend analysis, the Mann–Kendall test, and hot and cold spot analysis to deeply analyze the trend changes of ESs and the spatiotemporal evolution of CESI from 1999 to 2020. The integration of CESI and ES bundles enriches the research framework of spatial combinations of multiple ecosystem services. The

Data type	Variable name	Resolution	Source
China Land Cover Dataset	CLCD	30 m	Zenodo http://zenodo.org/record/8176941
Digital Elevation Model	DEM	30 m	Geospatial data cloud https://www.gscloud.cn/search
Normalized differential vegetation index	NDVI	1000 m	National Aeronautics and Space Administration https://search.earthdata.nasa.gov/search
Annual precipitation	PRE	1000 m	National Aeronautics and Space Administration https://search.earthdata.nasa.gov/search
Annual temperature	TEM	1000 m	National Aeronautics and Space Administration https://search.earthdata.nasa.gov/search
Annual potential evapotranspiration	PET	1000 m	National Aeronautics and Space Administration https://search.earthdata.nasa.gov/search
Soil sand content	SAND	1000 m	Food and Agriculture Organization of the United Nations http://dx.doi.org/https://doi.org/10.3334/ORNLDAAC/1247
Soil silt content	SILT	1000 m	Food and Agriculture Organization of the United Nations http://dx.doi.org/https://doi.org/10.3334/ORNLDAAC/1247
Soil clay content	CLAY	1000 m	Food and Agriculture Organization of the United Nations http://dx.doi.org/https://doi.org/10.3334/ORNLDAAC/1247
Population density	POP	1000 m	The World Pop Dataset https://www.worldpop.org/
Gross Domestic Product	GDP	1000 km	Resource and Environmental Science Data Platform http://www.resdc.cn/
Night Lights	NL	1000 m	Resource and Environmental Science Data Platform http://www.resdc.cn/

Table 1. Data sources.

Optimal Parameter Geographic Detector (OPGD) optimizes the spatial scale and zoning effects of geographic data, is not affected by human subjectivity, improves the quality and accuracy of research results, and accurately explores the key driving factors affecting ESs and CESI. MGWR is used to present the spatial heterogeneity of driving factors, deeply explore the relationship between ecosystem services and key driving factors, and deeply analyze the driving mechanism of ecosystem services from a spatial distribution perspective. Finally, the spatial distribution of the influencing factors of the comprehensive ecosystem service index and the distribution of hot and cold spots are used to divide the ecological functional zones. A study flow chart is illustrated in Fig. 2.

ESs assessment
Based on the ecosystem service assessment system constructed by the United Nations Millennium Ecosystem Assessment[38], adhering to the principles of scientificity, importance, and comprehensiveness, and closely combining with the actual situation of the Luo River Basin, four typical ecosystem service indicators, namely water yield(WY), carbon storage(CS), soil retention (SR), and habitat quality(HQ) were selected for in-depth analysis. These four services were evaluated using the InVEST model with calculation formulas provided in Table 2.

Non-parametric trend test
Theil-Sen (Sen) trend analysis is a reliable non-parametric statistical trend method that does not rely on specific parameters and can effectively handle data containing outliers or not conforming to a normal distribution, thereby reducing the impact of discrete data and measurement error[43]. The formula is:

$$\beta = \text{median}\left[\frac{ES_j - ES_k}{j - k}\right] \tag{5}$$

where β represents the trend of ESs, and ES_j and ES_k denote the time-series value of the sample in year j and year k ($j > k$). When $\beta > 0$, ESs are trending upward, and when $\beta < 0$, they are trending downward.

Without requiring the data to fit a particular distribution, the Mann–Kendall (MK) significance test is a non-parametric method for determining if monotonic trends exist in time-series data[44]. The formula are:

$$S = \sum_{i=1}^{n-1} \sum_{j=i+1}^{n} \sin\left(ES_j - ES_i\right) \tag{6}$$

$$\sin\left(ES_j - ES_i\right) = \begin{cases} -1, & ES_j < ES_i \\ 0, & ES_j = ES_i \\ 1, & ES_j > ES_i \end{cases} \tag{7}$$

$$Var\left(S\right) = \frac{n\left(n-1\right)\left(2n+5\right)}{18} \tag{8}$$

Fig. 2. The flow chart of the study. Software version: ArcMap 10.8, URL: https://www.esri.com/zh-cn/arcgi s/products/index. This map is produced based on the standard map with the review number GS(2024)0650, downloaded from the National Geographic Information Public Service Platform (website: https://www.tianditu .gov.cn/), and the base map has not been modified.

ESs	Calculation formula
Water yield	$Y(x) = \left(1 - \frac{AET(x)}{P(x)}\right) \cdot P(x)$ (1)
	Where $AET(X)$ denotes the annual actual evaporation (mm) per grid cell x and $P(x)$ denotes the annual precipitation (mm) per grid cell x[39,40]
Carbon storage	$C_{total} = C_{above} + C_{below} + C_{soil} + C_{dead}$ (2)
	Where C_{total} denotes the total carbon stock (t/hm^2), C_{above} denotes the above-ground carbon stock, C_{below} denotes the below-ground carbon stock (t/hm^2), C_{soil}(t/hm^2) denotes the soil carton stock, and C_{dead}(t/hm^2) denotes the dead organic carbon stock[41]
Soil retention	$SDR = RKLS - USLE = R \cdot K \cdot LS \cdot (1 - C \cdot P)$ (3)
	Where $RKLS$ denotes the potential total amount of soil erosion without vegetation cover and soil conservation measures ($t \cdot hm^2 \cdot yr^{-1}$), $USLE$ denotes the actual amount of soil erosion when vegetation cover and soil conservation measures are considered ($t\ hm^2\ yr^{-1}$), the management of vegetation cover factor is denoted by C, whereas the factor for soil and water conservation methods is represented by P[39]
Habitat quality	$Q_{xj} = H_j \cdot \left(1 - \frac{D_{xj}}{D_{xj}+k}\right)$ (4)
	Where H_j represents the habitat suitability of land use type j, D_{xj} represents the degree of habitat degradation of raster cell x in land use type j, k represents the half-saturation coefficient (the usual value is 0.5), and z represents the normalized constant (the usual value is 2.5)[42]

Table 2. Quantitative evaluation methods for ESs.

$$Z = \begin{cases} \frac{S-1}{\sqrt{\text{var}(S)}}, & S > 0 \\ 0, & S = 0 \\ \frac{S+1}{\sqrt{\text{var}(S)}}, & S < 0 \end{cases} \quad (9)$$

where S is the test statistic, which approximately follows a normal distribution; var(S) is the variance of S; and Z is the test statistic. If $|Z| \geq Z_{1-\frac{a}{2}}$, the original hypothesis is rejected and the trend is considered significant. With a significance level of $\alpha = 0.1$ and critical value $Z_{1-\frac{a}{2}} = \pm 1.65$ and with a significance level of $\alpha = 0.05$ and critical value $Z_{1-\frac{a}{2}} = \pm 1.96$ the time series passes the significance test at a 90% and 95% confidence level, respectively. Significant results were categorized as Very significant decrease ($\beta < 0$, $2.58 \leq Z$), Significant decrease ($\beta < 0$, $1.96 \leq Z < 2.58$), Relatively significant decrease($\beta < 0$, $1.65 \leq Z < 1.96$) Not significant decrease($\beta < 0$, $Z < 1.65$), No significant changes($\beta = 0$, $Z \leq 0$), Not significant increase($\beta > 0$, $Z < 1.65$), Relatively significant increase ($\beta > 0$, $1.65 \leq Z < 1.96$), Significant increase ($\beta > 0$, $1.96 \leq Z < 2.58$) and Very significant increase ($\beta > 0$, $2.58 \leq Z$).

The Sen slope is appropriate for trend analysis of lengthy time series since it is less sensitive to outliers and noise than other metrics[45]. However, Sen is not enable the determination of the significance of the trend of the series. The MK method is thus utilized to assess the significance of the data series owing to its better robustness, even if there are a few outliers in the data. Therefore, the combination of Sen + MK was determined to be the most suitable approach for a long time series analysis of ESs in the Luo River basin.

CESI
The CESI[17] is used to assess the provisioning capacity of multiple ESs in an integrated manner, emphasizing the balance and importance of services, with deficiencies in any single service significantly affecting the overall score. All of the ESs are normalized and transformed into a consistent dimensionless value to harmonize the units of various ESs. The formula is:

$$CESI = \prod_{\alpha=1}^{n} f(x, ES_\alpha, t) \quad (10)$$

where α is the type of ESs, n is the number of ESs, x is the value of the image element of ES_α at a given time point, t is the time variable, and $f(x, ES_\alpha, t)$ is the α ecosystem services of pixel x in the time period of t. The CESI ranges from 0 to 1, with higher scores representing a greater ability to supply multiple ESs.

Identification of ES bundles
A self-organizing map (SOM)[46] is an efficient unsupervised learning and data visualization method that plays a key role in research, especially in identifying and analyzing ES bundles at the township scale. Through the SOM, townships with similar ESs characteristics can be grouped into the same service bundle. In implementing the SOM, there is a similar need to standardize data on ESs to ensure that service bundles delineated in different years are consistent and comparable in scale. The SOM was built using the R 4.2.2 software's "kohonen" package[47].

Optimal parameter geographic detector
The GD is used to reveal spatially stratified heterogeneity and the extent of factors influence natural and socio-economic processes[48]. This model can quantitatively assess the contribution of different influencing factors to the spatial distribution pattern while detecting the extent to which the two factors interact on the dependent variable. As an improved method, OPGD[49] uses the "GD" package in R 4.2.3 to discretize continuous data, select appropriate discretization parameters, and accurately evaluate the explanatory power of driving factors[50]. The formula is:

$$q = 1 - \frac{\sum_{h=1}^{L} N_h \sigma_h^2}{N\sigma^2} = 1 - \frac{SSW}{SST} \quad (11)$$

where q values range from 0 to 1; the explanatory power increases with increasing value of q; h is the number of layers, and $h = 1,…L$ represents a stratification of ESs Y and impact factor X; N_h and N represent the number of samples and the total number of samples; σ_h^2 and σ^2 represent the discrete variance of ESs in stratum h and across the region; SSW and SST represent the sum of the intra-stratum variance and the total variance across the region.

The dynamic changes in ecosystem services are the result of the interaction between natural factors and human activities. Natural and climatic factors dominate the changes in ecosystem services, while socio-economic activities have a promoting or inhibiting effect on changes in ecosystem services. To accurately quantify the contribution of various driving factors, the representativeness, scientificity, and quantifiability of the factors were considered, covering 14 factors such as topography, climate, and socio-economic factors (Table 3) [31,34,51,52]. The OPGD model was used to further explore its contribution to the changes in ecosystem services in the Luo River Basin.

MGWR model
Ordinary least squares (OLS) regression ignores the spatial heterogeneity that exists among geographic elements, assuming that the spatial effects of explanatory variables are fixed[53,54]. GWR is effective in explaining spatial non-stationarity but neglects to account for differential scale effects of influencing factors[55]. MGWR combines

Category	Driver name	Abridge	Codes	Unit	Resolution	Datatypes
Natural factors	Elevation	DEM	X1	m	30 m	continuous
	Slope	SLOPE	X2	°	30 m	continuous
	Distance from the water system	WD	X3	–	1 km	categorical
	Normalized differential vegetation index	NDVI	X4	–	1 km	categorical
Climatic factors	Precipitation	PRE	X5	mm	1000 m	continuous
	Temperatures	TEM	X6	℃	1000 m	continuous
	Evapotranspiration	PET	X7	mm	1000 m	continuous
Soil composition	Soil sand content	SAND	X8	%	1 km	continuous
	Soil silt content	SILT	X9	%	1 km	continuous
	Soil clay content	CLAY	X10	%	1 km	continuous
Socio-economic factors	land use degree comprehensive index	LUDCI	X11	–	30 m	continuous
	Gross Domestic Product	GDP	X12	$10^3 \ km^{-2}$	1 km	continuous
	Population density	POP	X13	Pearson km^{-2}	1 km	continuous
	Night Lights	NL	X14	–	1 km	continuous

Table 3. Drivers of the ESs and CESI.

the spatial heterogeneity of GWR with the statistical advantages of traditional linear regression models. MGWR not only was the scale effect of the independent variable analyzed, but the flexibility and explanatory power of the model were further improved[56]. The MGWR model used in this study was constructed based on the MGWR 2.2 software developed by Oshan et al[57]. The adaptive bisquare was selected as the kernel function for weight matrix calculation, the Akaike information criterion (AICc) was used as the optimal bandwidth determination criterion, and SOC-f was used as the convergence criterion. The formula is:

$$y_i = \sum_{j=0}^{m} \beta_{bwj} \left(\mu_i, \nu_i \right) x_{ij} + \varepsilon_i \tag{12}$$

where y_i denotes the observed value of the dependent variable at sample point i; $\beta_{bwj} \left(u_i, v_i \right) x_{ij}$ denotes the coefficient of the independent variable j at sample point i, in which bwj represents the bandwidth used for the regression coefficient of the jth variable and x_{ij} denotes the observed value of the independent variable j at sample point i; and ε_i denotes the error term at sample point i.

Hotspot analysis
The hotspot analysis[58] (Getis-Ord Gi*) tool in ArcGIS 10.8 software was used to identify the aggregation degree and spatial distribution characteristics of ecosystem services and their comprehensive index in the Luo River Basin. The township administrative unit is used as the basic analysis unit to ensure that the analysis results are consistent with the policy implementation unit. The fixed distance band method is used to construct the spatial weight matrix, and the Euclidean distance is used to calculate the spatial relationship. Hotspot analysis, by analyzing the calculated z-scores and p-values, can obtain the locations where high-value or low-value features are clustered in space, based on which the aggregation of significant hotspots and coldspots can be identified.

$$G_i^* = \frac{\sum_{j=1}^{n} W_{ij} X_j - \overline{X} \sum_{j=1}^{n} W_{ij}}{S \sqrt{\frac{n \sum_{j=1}^{n} W_{ij}^2 - \left(\sum_{j=1}^{n} W_{ij}^2 \right)^2}{n-1}}} \tag{13}$$

where $Gi*$ is equivalent to the z-score. The higher the z value, the tighter the high-value clustering; the lower the z value, the tighter the low-value clustering; W_{ij} is the spatial weight between township unit i and township unit j; X_j is the attribute value of township unit j; $\overline{X}$ is the overall average; n is the number of research units; S is the standard deviation. The z value is used to distinguish the spatial agglomeration characteristics: hotspot** (≥ 2.58); hotspot* [1.96, 2.58); hotspot [1.65, 1.96); Not significant (− 1.65, 1.65); coldspot (− 1.96, − 1.65]; coldspot* (− 2.58, − 1.96]; coldspot** (≤ − 2.58).

Results and analysis
Spatiotemporal characterization and hotspot analysis of ESs
From 1999 to 2020, variations in ESs trends in the Luo River basin were examined using the Sen + MK trend significance test, multi-year averages, and cold/hotspot analysis (Fig. 3). WY, CS, and SR showed an overall increasing trend in spatial distribution, while HQ showed a significant downward trend. Specifically, the area with an increasing trend in WY accounts for 99.81%. The growth rate is more significant and above in the northern edge and northwest of the basin, accounting for 15.4% of the study area. The multi-year average revealed that
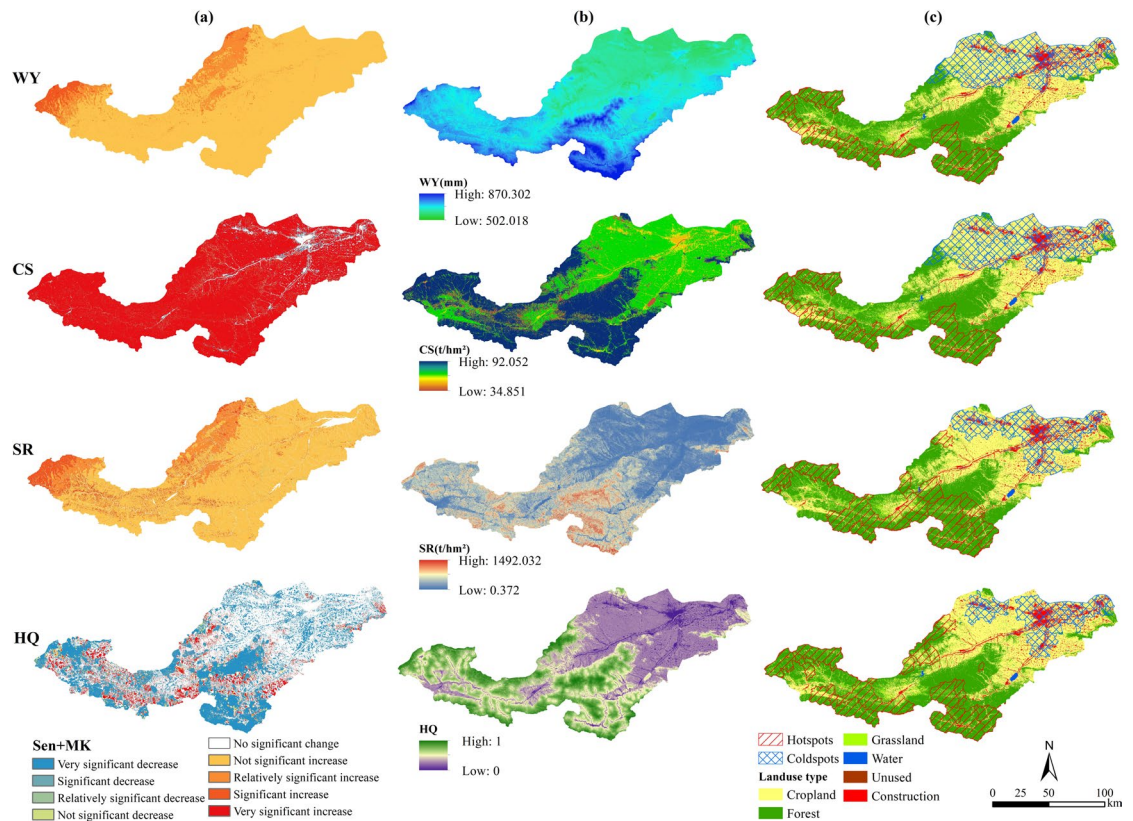
Fig. 3. (**a**) Trend changes, (**b**) multi-year average, and (**c**) hotspot analysis of ESs in the Luo River basin. Software version: ArcMap 10.8, URL: https://www.esri.com/zh-cn/arcgis/products/index. This map is produced based on the standard map with the review number GS(2024)0650, downloaded from the National Geographic Information Public Service Platform (website: https://www.tianditu.gov.cn/), and the base map has not been modified.

WY had a geographical distribution with high levels in the basin's southwest and low values in its northeast. The hotspots of WY were found to be mainly concentrated in the southern upstream areas of Luanchuan County, Luonan County, and Huazhou District, while the cold spots were found in the northeastern part of the research area. In terms of CS, 90.52% of the study area showed an increasing trend, of which 88.7% showed a significant increasing trend. The distribution of hot and cold spots in CS is similar to that of WY pattern in space, with a certain spatial correlation. Hot spots are distributed in upstream forest areas, while cold spots are distributed in areas with high human activity intensity such as cities and cultivated land. In terms of SR, 92.3% of the areas showed an upward trend, with only a few areas exhibiting a significant upward trend, while 72.8% of the upward trends were not significant. High SR values were mainly concentrated in Luanchuan County, Lushi County, and the southern edge of the basin, where SR growth is most significant. This distribution of hotspots was generally consistent with that of CS. On the other hand, the cold spot locations were mostly found in Luoyang's important urban centers, where SR growth is relatively weak. In contrast to the changes in ESs described above, we found a significant declining trend in HQ across the entire basin. With just 7.5% of the regions showing a significant increase and 34.6% of the regions showing a significant decrease. The hot and cold spot distribution pattern of HQ is similar to that of SR. The high-value areas of HQ are mainly concentrated in the southwest of the basin, while the low-value areas are mainly distributed in the northeast. The construction of forests and grasslands in the upstream areas promoted the improvement of habitat quality, but due to the influence of urban expansion, a large amount of cultivated land was occupied, which seriously damaged the habitat quality, and ultimately caused the overall HQ of the basin to show a significant downward trend. By superimposing the hot and cold spots of ESs with land use, it was found that the hot spots of ESs were mainly concentrated in lush woodlands and scattered grassland areas, while the cold spots were mainly distributed in farmlands and construction land areas in the northeast.

Figure 4 displays the characteristics of annual fluctuations in ESs in the Luo River basin between 1999 and 2020. WY showed obvious fluctuating and changing characteristics, although the overall trend was slightly upward, with an annual average value of 614.89 mm. During the study period, WY dropped to a historic low of 414.96 mm in 2001 and then climbed to a peak of 899.67 mm in 2003. The average annual growth rate was 4.71%, with the highest growth rate of 64.49% detected in 2002–2003. CS showed the same fluctuating upward trend with an annual average value of 84.05 t/hm²; the lowest value occurred in 2012 at 83.69 t/hm² and the highest value occurred in 2020 at 84.88 t/hm². CS values gradually increased from 2003 to 2007; however, there
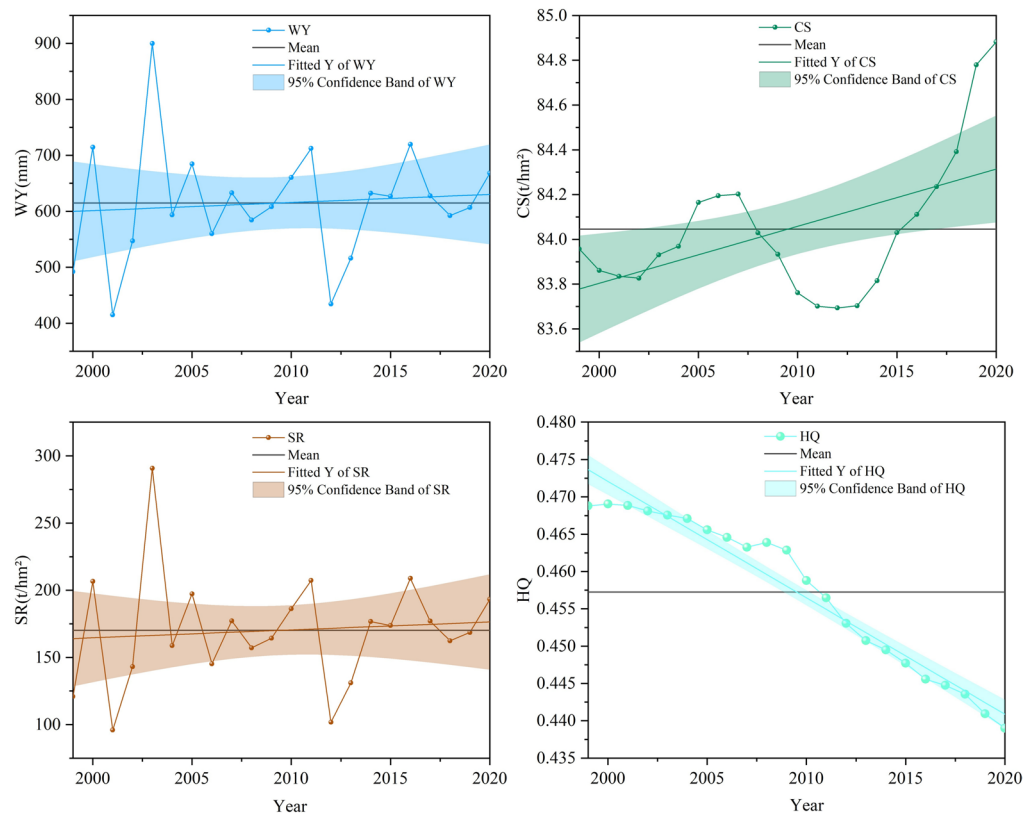
Fig. 4. Inter-annual variation of ESs in the Luo River basin.

was a downward trend from 2007 to 2012, followed by another rebound. The average annual growth rate was found to be 0.05%, with the largest growth rate of 0.46% detected in 2018–2019. The inter-annual variation of SR demonstrated a slow fluctuating upward trend, similar to that of WY, with an annual average value of 170.19 t/hm². Specifically, SR was the lowest at 95.94 t/hm² in 2001 and peaked at 290.86 t/hm² in 2003. The average annual growth rate was 8.97%, with the highest growth rate of 103.20% detected in 2002–2003. HQ showed a significant downward trend despite inter-annual variation, with a multi-year mean value of 0.4572 and a relatively small overall range of variation between 0.4390 and 0.4691. There has been a notable declining tendency, with an average yearly rise of − 0.31% and an overall increase of − 6.35% from 1999 to 2020.

Spatiotemporal distribution of the CESI

CESI, as a key indicator for comprehensively evaluating the supply capacity of multiple ecosystem services, reveals the spatial heterogeneity of the supply capacity of the Luo River Basin. The CESI value in the northeast of the basin is relatively low, and the supply capacity in the southwestern edge is strong. The high-value areas are concentrated in the southern edge of the basin, such as Luanchuan County, and are mostly mountainous and hilly areas. WY, CS, SR, and HQ serve a synergistic gain mechanism, superimposed with ecological protection and restoration measures implemented by humans. For example, the GFGP has promoted the conversion of farmland into forest land, significantly increased forest coverage, strengthened vegetation carbon sequestration, soil conservation, and other functions, and effectively reduced soil erosion. With good natural conditions and effective protection measures, a strong ESs supply is maintained, which promotes the formation of high CESI values. In contrast, downstream urbanized areas, such as the townships under the jurisdiction of Luoyang and Zhengzhou, are affected by the expansion of construction land and high-intensity human activities, which limits the supply of ecosystem services and leads to lower CESI values.

Following the natural breakpoint method, the CESI at the township scale in the watershed was categorized into five intervals: high-value region (0.205–0.404), relatively high-value region (0.101–0.205), median region (0.049–0.101), relatively low-value region (0.017–0.049), and low-value region (0–0.017) (Fig. 5). The high-value regions are dispersed less; Similar to the distribution of single ESs, the comparatively high-value regions are located in the southern portion of the middle reaches of the watershed; the median region is immediately north of the relatively high-value region; the relatively low-value region is located north of the headwaters; and the remaining area constitutes the low-value region, which is mainly the distribution area of cropland and built up land, where CESI values decrease continuously from south to north.

The analysis of hot and cold spots revealed that the spatial distribution of the CESI and its changes show a significant trend of local clustering, and the overall alterations are comparable to the hot and cold spots' spatial distribution in WY, CS, SR, and HQ. Changes in most areas were not significant, and the percentage of insignificant areas exceeded 60% of the research area over the years, reflecting the stability of ESs supply.
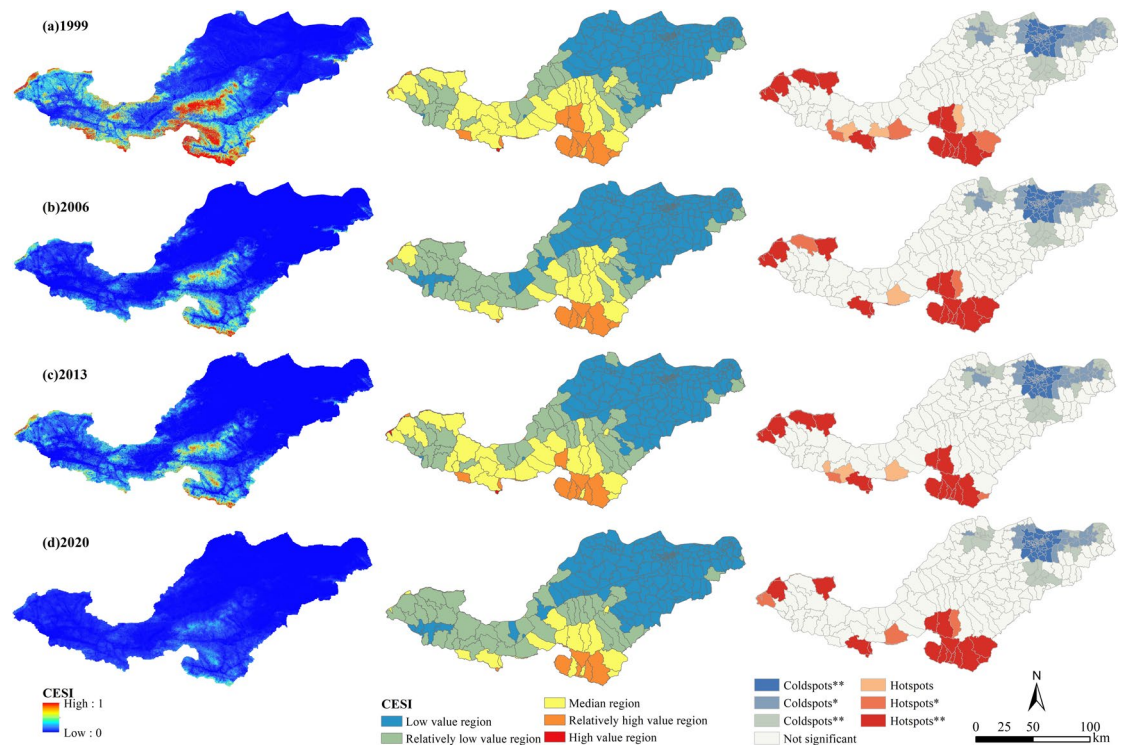
Fig. 5. Characterization of changes in CESI and analysis of hot and cold spots. Software version: ArcMap 10.8, URL: https://www.esri.com/zh-cn/arcgis/products/index. This map is produced based on the standard map with the review number GS(2024)0650, downloaded from the National Geographic Information Public Service Platform (website: https://www.tianditu.gov.cn/), and the base map has not been modified.

The restoration of upstream forest land has significantly improved water production, carbon storage, and other services, creating an ecosystem service hotspot, while downstream cities have formed ecosystem service cold spots due to expansion. The ecosystem services of cultivated land in the central region do not vary much in space. At the same time, soil erosion control and non-point source pollution coexist in the transition zone between forest and cultivated land, and the spatial aggregation of service values is not significant. Specifically, the hotspot areas in 1999 were mainly concentrated in the townships under the jurisdiction of Luanchuan County and in the southwestern part of Lushi County, which are high ESs provision areas. However, it was discovered that the cold spot locations are situated in places like Luoyang's central metropolitan area, which is comparatively more impacted by human activity and has a lower capacity to supply ESs. The confidence level of hotspot areas in Luanchuan County increased in 2006, showing a further increase in the ESs supply of the region; the number of hotspot areas in the southern part of the watershed decreased, along with a slight decrease in cold spot areas. In 2013, the 95% confidence level hotspot area shifted to Luonan County in the northwest and the hotspot area in Danfeng County increased, reflecting the spatial redistribution of ESs supply; however, the cold spot area did not undergo substantial change at this time. In 2020, the hotspot area moved south again, while the cold spot area decreased further. Therefore, when evaluating the supply of ESs, it is necessary to take into account the level and potential capacity of each service to more accurately grasp the overall situation and development trend of regional ecosystems.

Distribution and characterization of ES bundles

We further analyzed the interdependence between ESs in the Luo River basin and explored the structure of ESs components in different regions. At the township scale, four ES bundles types were identified through SOM analysis, namely ecological protection bundle (B1 bundle), integrated ecological bundle (B2 bundle), key synergistic bundle (B3 bundle), and urban center bundle (B4 bundle) (Fig. 6). Among these four service bundles, bundle B1 is mainly characterized by the provision of lower levels of CS and HQ, and its distribution is mainly concentrated in croplands in the lower portions of the watershed in the northeast, especially in the cities of Yima and Luoyang. In 1999, the area proportion was roughly 28.96%. From 1999 to 2020, the area changed, exhibiting an increasing tendency that was followed by a declining trend. The B2 bundle includes a variety of excellent services, including high levels of WY, CS, SR, and HQ, and its distribution is dominated by woodlands, which feature prominently in the southern part of the upper watershed. However, its area share has experienced significant changes, with an overall sharp decline from 66.55% in 1999 to 13.96% in 2020. The specific transformation showed a significant decrease followed by a slow increase in the trend, with a particularly notable decline from 1999 to 2006. The land use types in the distribution area of the B3 bundle are mainly forest and grassland, and their CS, SR, and HQ services all have strong supply. This service bundle is concentrated
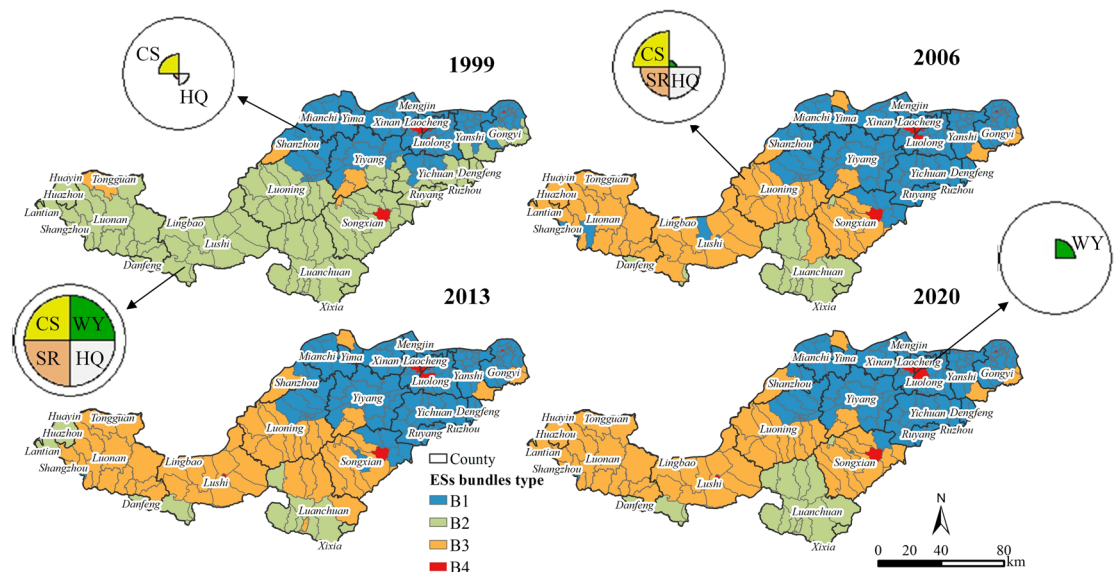
Fig. 6. Spatial–temporal distribution of ES bundles. Software version: ArcMap 10.8, URL: https://www.esri.com/zh-cn/arcgis/products/index. This map is produced based on the standard map with the review number GS(2024)0650, downloaded from the National Geographic Information Public Service Platform (website: https://www.tianditu.gov.cn/), and the base map has not been modified.

in the hilly, mountainous terrain in the northern part of the headwaters, with a significant increase in area share from 3.54% in 1999 to 48.01% in 2020, showing an overall increasing trend. Bundle B4 is characterized by providing a low level of WY and is distributed within bundle B1, which is mainly the construction land in Luoyang City's central urban region. With rapid urbanization, this area continues to expand, reflecting the delicate balance between urban development and ESs.

In terms of the mutual transfer of service bundles, in 1999, bundle B1 was concentrated in the downstream zone of Luoyang River, bundle B2 was located in the watershed's upper reaches, bundle B3 covered a relatively small area, and bundle B4 firmly occupied the center of Luoyang's urban area. Over time, the distribution pattern of service bundles changed significantly from 1999 to 2006. The watershed area covered by bundle B1 in the upper Luo River basin increased by 2,272.27 km^2, representing a significant increase mainly due to the transformation of bundle B2. At the same time, the B3 bundle showed a dramatic expansion of 8080.06 km^2, in which the transformation area from the B2 bundle to the B3 bundle became the key implementation site of the ecological management project of the fallow forest. Bundle B1 is located in a township that exhibits low synergistic supply capacity in terms of CS and HQ, although some of the B1 bundles have transformed into B4 bundles.

The implementation of the GFGP has significantly contributed to the ecological restoration of the Luo River Basin. Remote sensing monitoring data showed that 76.97% of the area in the basin showed an improving trend in vegetation cover between 2000 and 2020[59]. In 2013, there was a small increase of 583.03 km^2 in the area of the B3 bundle, which was transformed from part of the B1 and B2 bundles, while the area of the other bundles showed relatively minimal change. Between 2013 and 2020, the B2 bundles area south of the middle reaches of the watershed expanded by 706.47 km^2, marking a significant improvement in the comprehensive high provisioning capacity of ESs in the Luo River basin. Although the number of townships has not changed, this positive change reflects the significant results of ecological restoration efforts. It is worth noting that bundle B4 has consistently been concentrated in areas of rapid urbanization, which has significant negative impacts on downstream areas, resulting in relatively low levels of ESs provided by bundles B1 and B4. Therefore, differentiated management strategies should be implemented through the classification of ES bundles for different target townships.

Drivers of ESs

Analysis results of OPGD

Before applying OPGD and MGWR, variable selection was controlled by double criteria. Ordinary least squares regression (OLS) was used to calculate the variance inflation factor (VIF), with VIF > 7.5 as the multicollinearity elimination threshold[60]. A significance test (99% confidence level) was performed based on the Spearman correlation coefficient (applicable to non-normal distribution and data containing extreme values[61]), and variables that failed to pass statistical significance verification were excluded. The histogram analysis using SPSS software showed that the distribution of driving factor data showed complex nonlinear characteristics and deviated from normality (Fig. 7). The explanatory variables finally selected met both collinearity constraints and statistical significance requirements.

To avoid subjective human influence, the OPGD is applied when discretizing continuous data[49], which can further extract information contained in geographic features and spatial explanatory variables[62]. Using 2020 as an example, among the variables that passed the significance test (Fig. 8), PRE is the key driving factor of WY
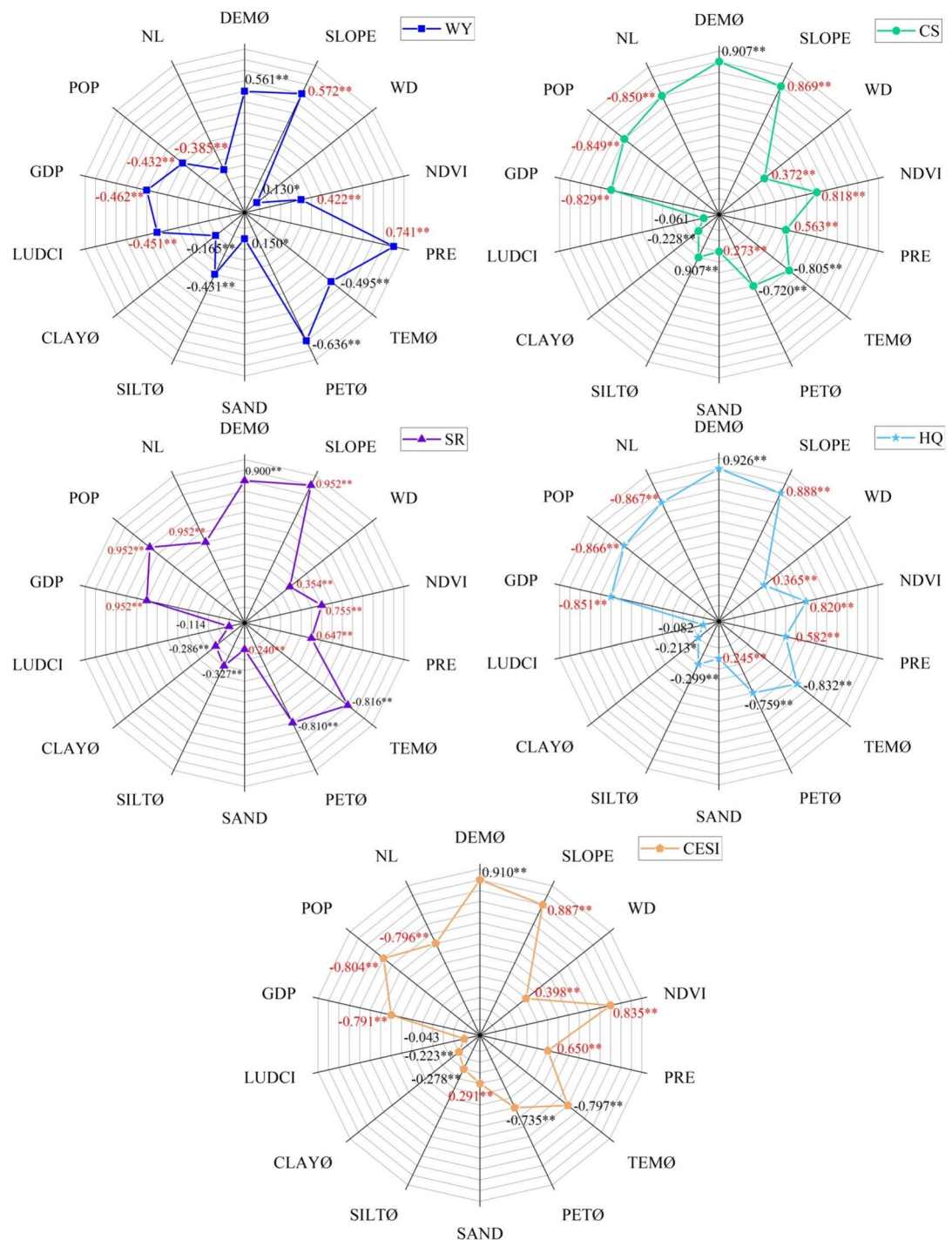
Fig. 7. Spearman correlation coefficients of important drivers of ESs in the Luo River basin in 2020. Note: ** and * indicate that the factor passes the 99% and 95% confidence level tests, respectively; ∅ indicates that it does not pass the diagnostic of covariance; and red indicates the selected main drivers.

(q = 0.7543), and its interaction with NDVI explanatory power on WY rises to q = 0.8608 (Fig. 9), exceeding the single factor effect. This nonlinear synergistic mechanism suggests that vegetation cover plays a dynamic regulatory role in the process of converting rainfall into water yield. LUDCI has the weakest independent explanatory power for WY (q = 0.2683). CS was mainly driven by NDVI (q = 0.8001), and the explanatory power of the interaction between SLOPE and NDVI (q = 0.9387) on CS was nearly 1.2 times that of the single NDVI effect. This indicates that vegetation restoration in steep slope areas promotes carbon sequestration through terrain-vegetation interaction. Both SR and HQ show that natural factors dominate, and SLOPE has the strongest explanatory power for SR (q = 0.8853), and its interaction with PRE further strengthens this effect (q = 0.9357). HQ was mainly affected by SLOPE (q = 0.8739), and the interaction between SLOPE and NDVI
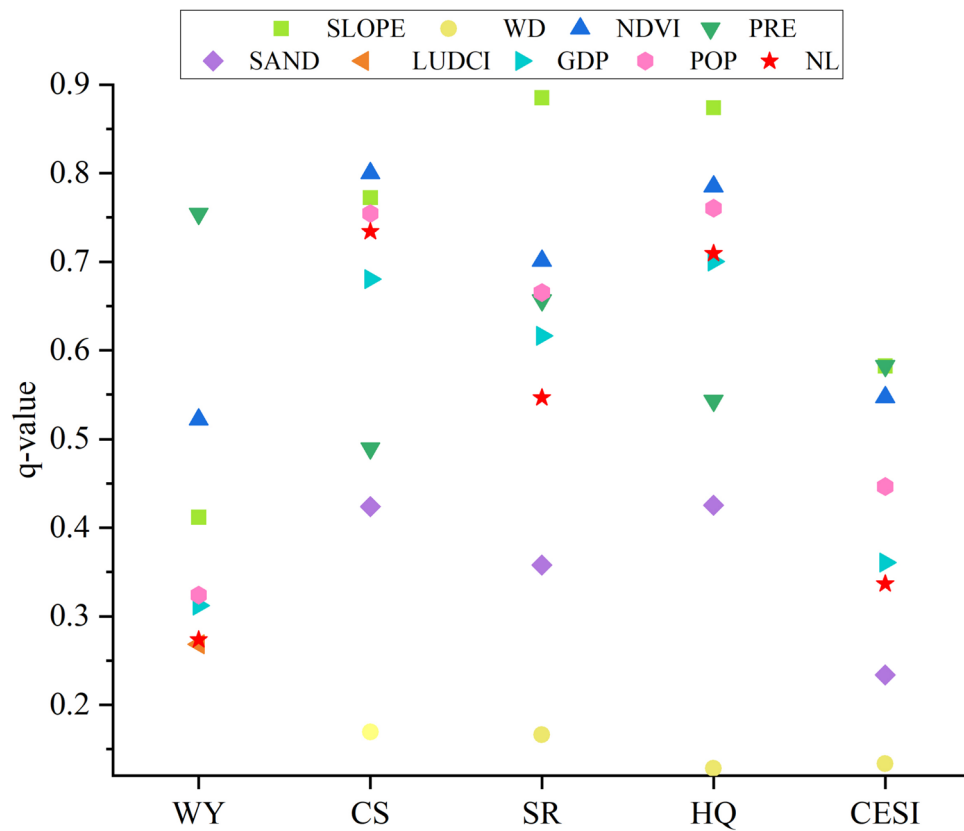
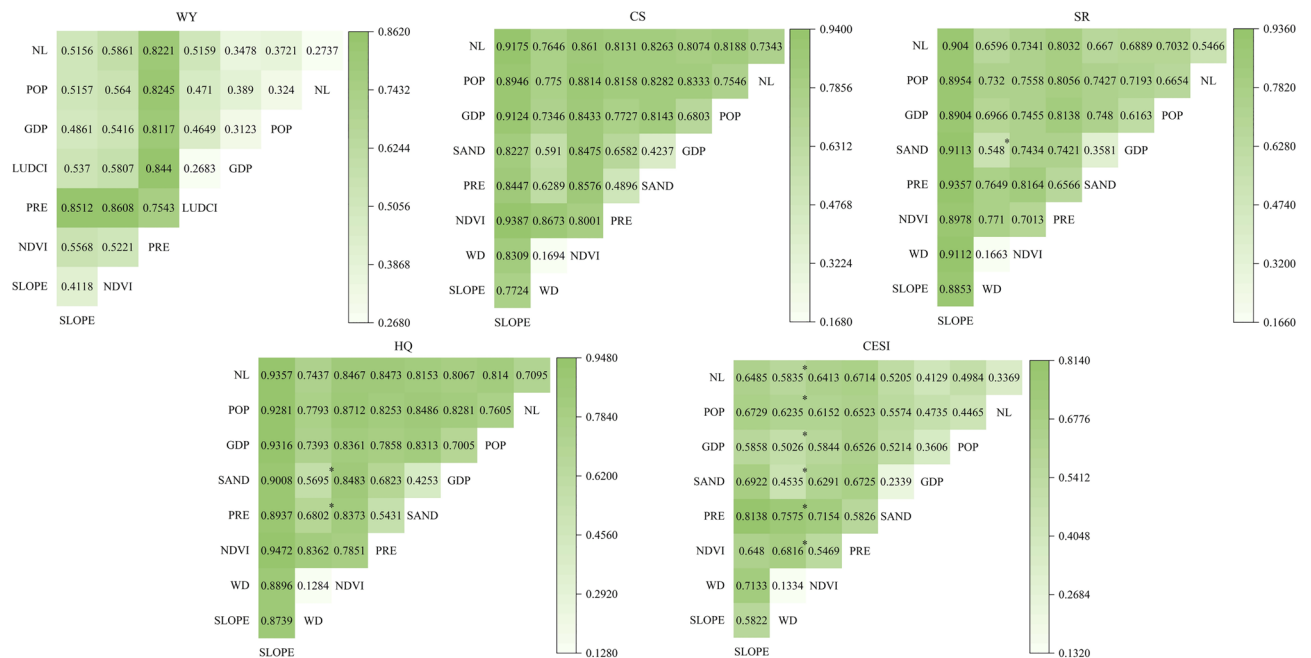**Fig. 8**. OPGD single factor detection results.

Fig. 9. OPGD factor interaction detection results. Note: * indicates that the interaction type is the nonlinear enhancement.

reached the maximum explanatory level (q = 0.9427). It is worth noting that WD has the weakest influence on CS, SR, and HQ (q = 0.1694, 0.1663, 0.1284), and the influence of location factors is small. CESI is significantly affected by natural climate factors, among which the explanatory power of PRE (q = 0.5826) exceeds that of all socioeconomic variables, and the interaction between SLOPE and PRE further dominates the change of CESI (q = 0.8138). In all interactions, the factors' interactive effects exceed the explanatory power of a single factor and show bi-enhancement or nonlinear enhancement characteristics.

Spatial distribution of MGWR determined dominant drivers
To ensure the superiority of the MGWR model, it was analyzed in comparison with OLS and GWR. The models were compared by using the adjusted coefficient of determination (Adj. R^2) and the Akaike information criterion (AICc). To more accurately evaluate the fit of the model, the adjusted R^2 must be less than or equal to R^2. MGWR (Adj.R^2: 0.90, R^2: 0.92, taking WY as an example, the same below) and GWR (Adj.R^2: 0.78, R^2: 0.81) are compared with the commonly used linear regression model (Adj.R^2: 0.43, R^2: 0.44). The model accuracy results show (Table 4) that the OLS model has the highest AICc value and the lowest Adj.R^2 value, while the MGWR model exhibits the lowest AICc and the highest Adj.R^2, and the model parameters of GWR are in between the two. The MGWR model has a greater model fit advantage (Adj R^2) than the GWR and OLS models, further demonstrating that the model performed best when it came to illuminating how important drivers affected the dependent variable's spatial variation (Table 4). Therefore, based on the OPGD analysis, MGWR was utilized to explore the spatial distribution of the dependent variable by the primary drivers with impact rankings in the top three.

After classification into five categories according to the natural breakpoint method (Fig. 10), the positive effect of PRE on WY was found to be significant, and this effect was particularly pronounced in the northern regions. The impact of the NDVI on WY was bidirectional, and the positive influence coefficient was mainly concentrated in the central part of the watershed, indicating that the increase of vegetation cover would significantly enhance the water production capacity. SLOPE has a significant positive impact on WY. The increase in the slope in the upstream of the basin accelerates surface runoff, reduces infiltration, and increases runoff. The slope of the hardened surface area downstream further intensifies runoff, inhibits infiltration, and increases water production. The NDVI showed a positive influencing effect on CS in the lower portion of the watershed, with the effect progressively growing from west to east. This suggests that the region's plant growth positively influences CS growth. SLOPE had a similarly positive impact effect on CS, which was centered around the midstream region, with a progressively higher contribution from the outside in. The negative influence of POP was significant on CS, and its inhibitory effect gradually increased in the western part of the watershed. SLOPE showed a positive influence impact on SR, and the facilitating effects gradually increased from the northeast to the southwest. In the middle of the basin, the NDVI also had a positive impact on SR, and this promotion effect grew progressively from the north to the south. The impact of POP on SR showed positive and negative bidirectional effects, with an inhibitory effect in the upstream area and a shift to a facilitating effect in the downstream area, demonstrating the complex impact of POP in different watershed areas. SLOPE exerted a significant positive influence on HQ, and the promotion effect gradually increased from the east to the west, indicating that the ecological environment in the upstream area improved with upward elevation. The NDVI also exhibited a positive impact on HQ in the downstream part of the watershed, with its contribution increasing gradually from the west to the east. However, POP had a negative effect on HQ, and this inhibitory effect spread throughout the watershed, indicating varying degrees of damage to HQ from human activities.

Overall, the drivers of ESs in the Luo River basin show complex spatial variability, with PRE positively influencing effects on the CESI in the north, especially in cropland areas. This indicates that the precipitation in the region positively contributes to the CESI and significantly enhances the CESI level. From northeast to southwest, SLOPE's positive effect on the CESI grew progressively. Furthermore, there was a significant positive effect of the NDVI on the CESI, which increased progressively from the north to the south, suggesting that the CESI was positively impacted by the improvement in vegetation quality.

Partitioning strategy for CESI, ES bundles, and driver integration

In advancing ecological engineering projects, scientific planning and precise management should be strengthened. By accurately understanding the changing trends of ESs in the Luo River basin, we can comprehensively enhance

Model accuracy		WY	CS	SR	HQ	CESI
OLS	AICc	2906.3536	144.3765	1555.6365	− 624.2709	− 1181.9974
	R^2	0.4427	0.9207	0.9057	0.9158	0.5423
	Adjusted R^2	0.4287	0.9184	0.9030	0.9134	0.5292
GWR	AICc	2646.1258	83.6474	1428.4418	− 754.9975	− 1344.954
	R^2	0.8086	0.9454	0.9484	0.9546	0.7792
	Adjusted R^2	0.7822	0.9376	0.9412	0.9481	0.7479
MGWR	AICc	2476.5226	− 47.4825	1359.0155	− 844.1769	− 1434.3544
	R^2	0.9220	0.975	0.963	0.9700	0.8460
	Adjusted R^2	0.9020	0.968	0.956	0.9640	0.8250

Table 4. MGWR with OLS and GWR model parameter comparison.

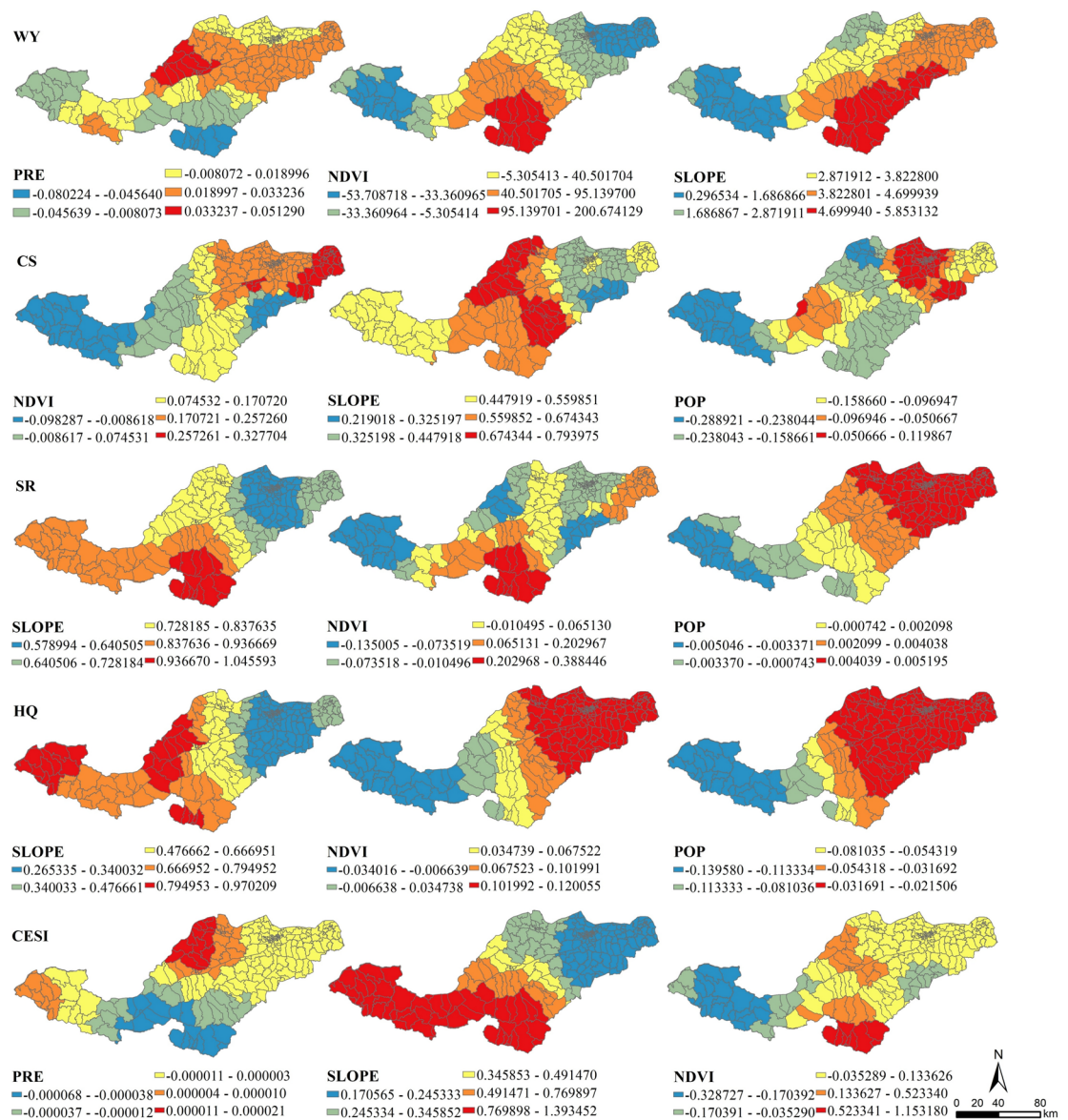**Fig. 10**. Spatial distribution of the main drivers of ESs in the Luo River basin. Software version: ArcMap 10.8, URL: https://www.esri.com/zh-cn/arcgis/products/index. This map is produced based on the standard map with the review number GS(2024)0650, downloaded from the National Geographic Information Public Service Platform (website: https://www.tianditu.gov.cn/), and the base map has not been modified.

their service levels, providing strong support for sustainable environmental development. Based on the CESI at the township size, we divided the area into five intervals using the natural breaks method (Fig. 5). Combining this with ES bundles (Fig. 6), we conducted primary functional zoning at the county scale (Fig. 11). The basin was divided into the upper-middle and middle-lower reaches using the K-means clustering approach. The upper-middle reaches are mainly forested areas with high levels of CESI and ES bundles, resulting in high ESs provision. In contrast, the middle-lower reaches, dominated by farmland and construction land, have relatively low ESs provision due to frequent human activities. The regional variability of ESs drivers was comprehensively considered, based on the primary driving variables of PRE, SLOPE, and the NDVI. Through the K-means clustering method, the secondary zoning was further implemented and divided into four secondary zones: namely, Ecological Protection Zone (I-1): located in mountainous and hilly areas with steep slopes, abundant precipitation, and high vegetation coverage, and high ecosystem service supply capacity. ESs are promoted by the NDVI and SLOPE, while slightly inhibited by PRE. Ecological Construction Zone (I-2) has a complex terrain, with the elevation gradually decreasing from west to east, leading to a high risk of soil erosion. SLOPE and PRE have a positive impact on ESs, while the NDVI has a negative impact. Cultivated Land Management Zone (II-1) is concentrated in valley alluvial plains and intermountain basins, serving as the primary agricultural land of the basin; its ESs provision is relatively low. Urban Construction Zone (II-2) is located in Luoyang's central metropolitan area, with a limited supply capacity of ESs. The NDVI and SLOPE have a facilitating effect and
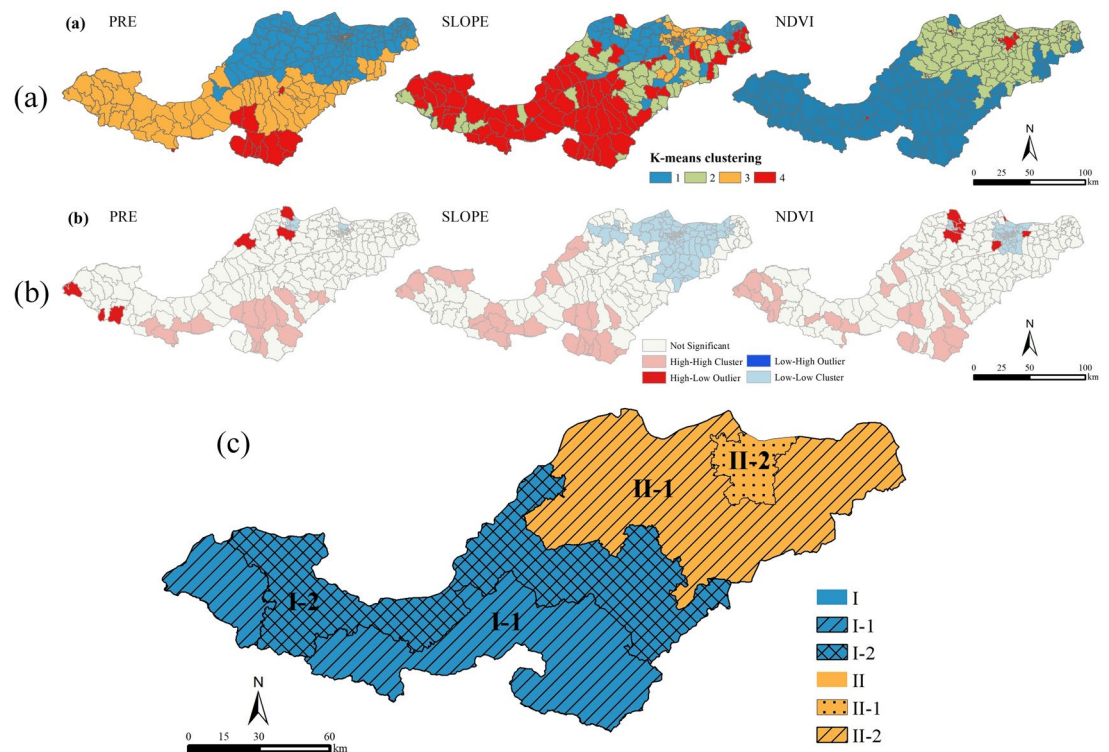
Fig. 11. Functional zoning of ESs in the Luo River basin: (**a**) K-means clustering of key driving factors, (**b**) Local Moran's I of key driving factors, and (**c**) distribution map of primary and secondary zoning in the basin. Software version: ArcMap 10.8, URL: https://www.esri.com/zh-cn/arcgis/products/index. This map is produced based on the standard map with the review number GS(2024)0650, downloaded from the National Geographic Information Public Service Platform (website: https://www.tianditu.gov.cn/), and the base map has not been modified.

PRE has an inhibiting effect. This thorough subdivision gives acceptable suggestions for achieving sustainable development and ecological preservation in the Luo River basin in addition to offering a scientific foundation for spatial planning and management at the township level.

Discussion
Characterizing changes in ESs
The spatiotemporal evolution characteristics of ecosystem services in the Luo River Basin showed that WY, CS, and SR all showed a fluctuating growth trend, which was closely related to the implementation of the GFGP[63]. Research results show that the project of returning farmland to forest has effectively increased watershed water yield, carbon storage, and soil conservation by increasing vegetation cover[64,65]. Specifically, the upstream area has a strong CS capacity due to its vast forest area and vigorous vegetation growth, while the well-developed plant root system further enhances the SR function. The downstream area is disturbed by human activities such as urbanization, industrialization, and overexploitation of cultivated land resources, and the vegetation coverage is low, resulting in limited CS increment. High-intensity human activities have led to the continuous degradation of HQ, and its downward trend is consistent with the conclusion of Hisano et al[9]. The above results reveal the differentiated impacts of natural recovery and human disturbance on ecosystem services and provide a theoretical basis for watershed zoning management. WY, CS, SR, and HQ showed convergent characteristics in spatial distribution. The mountainous and hilly areas in the upper reaches of the basin formed high ESs value clusters due to the rich forest resources. The increasing expansion of forest coverage and the increase in vegetation density drive multiple ecological gains. Forests fix large amounts of carbon through photosynthesis[66], and their carbon storage capacity is significantly improved. Vegetation intercepts rainfall, stabilizes soil particles using the roots of trees and vegetation, and reduces the risk of soil erosion[67,68]. The accumulation of biomass forms a heterogeneous habitat structure, storing more biomass to provide a diverse habitat, providing a key carrier for maintaining biodiversity, and continuously optimizing the upstream habitat quality index. In high-altitude areas, abundant orographic rainfall is formed due to the influence of climate, providing sufficient water sources and enhancing water production capacity[69]. The combination of topographic and climatic features ensures that the region has significant supply advantages in terms of water production.

Combined analysis of the CESI and ES bundles reveals the spatial features of ESs
CESI was used to evaluate the overall supply level of ESs in the Luo River Basin. However, relying solely on CESI cannot fully characterize the spatial differentiation of multiple ESs. The innovative combination of CESI

and ES bundles can more accurately reveal the distribution characteristics of multiple ecosystem services at the spatial level. The CESI value in the lower reaches of the Luo River Basin is significantly lower than that in the B1 and B4 bundles. This result is mainly due to the combined effects of accelerated urbanization and increased intensity of human activities, which have led to a significant degradation of ecosystem services. The upstream area presents a high CESI value, and this area has a strong ability to provide various ecosystem services, and its synergistic gain effects of CS, SR, and HQ are significant. Although the rugged terrain upstream and the intensity of surface runoff increase the risk of soil erosion[68]. Ecological projects such as GFGP can effectively curb soil erosion and enhance soil stability by increasing vegetation coverage, but the increase in evaporation caused by large-scale afforestation has an inhibitory effect on WY in the region[70,71]. To avoid potential problems caused by excessive afforestation, scientific planning is essential while encouraging the building of ecological projects. Targeted development and implementation of ESs management strategies, and thus promote the comprehensive improvement of ESs in the Luo River Basin.

Integrating the OPGD and MGWR for spatial visualization of ESs drivers

This study used OPGD and MGWR methods to systematically and comprehensively analyze each driver's influence on the dependent variable. The findings demonstrated that soil composition and socioeconomic factors have a smaller impact on ESs than do natural and climatic factors. The results are consistent with those of Chen et al., and Alcamo et al[72,73]. PRE had the most significant effect on WY and showed a significant positive effect, consistent with the findings of Jia et al[74]. As rainfall increases, more water is available for vegetation uptake and soil storage, which in turn is converted into surface and groundwater, thus effectively boosting water production. The interactive effect between NDVI and PRE on WY was particularly significant, and the results were consistent with the conclusions of Song et al[75]. This interaction not only promotes the growth of vegetation and improves water use efficiency, but also enhances the storage capacity of soil moisture. The NDVI was also identified as a crucial factor affecting CS, in accordance with the conclusions of Li et al[76]. In particular, the positive contribution of the NDVI to CS was significant in the downstream area, and the total plant biomass in the high vegetation cover area increased, which in turn enhanced CS. The interaction between SLOPE and the NDVI had a particularly strong effect on CS, and the results are consistent with the conclusions of Wang et al[35]. By influencing the degree of soil erosion, the growth of vegetation is indirectly affected, consequently influencing the pattern of CS and its distribution.

Among the many factors affecting SR, the contribution of SLOPE was determined to be the most significant, in line with the findings of Fang et al[77]. From the watershed's northeast to southwest, the SLOPE effect's beneficial effects grew progressively. The interaction between SLOPE and PRE plays the most critical role in SR[78]. Moderate slopes help surface water to drain away quickly, reducing the amount of time water is retained on the surface, which in turn reduces the risk of water and wind erosion. Areas of high topographic variation and surface runoff exacerbate erosion phenomena[28]. Although increased precipitation and slope have resulted in a decrease in soil retention stability in the study area, the increase in woodland and perennial crops has improved overall stability[79]. It was discovered that the most significant factor influencing SR was the interaction between SLOPE and PRE. The simultaneous increase of slope and rainfall leads to a significantly faster runoff rate and increased water impact, which in turn accelerates the process of soil erosion. In addition, the topographic factor SLOPE was significantly correlated with HQ, in line with the conclusions of Sun et al[80]. Its positive facilitation effect increased gradually from the east to the west. In areas with steep slopes, there is less threat to HQ due to the difficulty of building land development and the comparatively lower level of human activity. Simultaneously, the area has become much more forested, thereby enhancing HQ. The interaction between SLOPE and the NDVI had the most significant effect on HQ[75]. In areas of relatively gentle slopes, there is more anthropogenic disturbance, which severely affects the structure and stability of the habitat.

Natural and climatic factors dominated the impact of the CESI, which far outweighed the contributions of socio-economic factors. Among them, PRE had the most significant impact on the CESI, especially in the downstream cropland area, and its influence involves water supply, ecosystem structure, and biological survival at many levels. The interaction between SLOPE and PRE perturbs ecological processes and thus has a significant effect on CESI performance. Notably, the explanatory power of the above interactions far exceeded the strength of the one-way effects, and the interactions all showed either a bi-enhancement or nonlinear enhancement pattern. Therefore, to properly and thoroughly comprehend the influence mechanisms of natural and climatic elements, it is imperative that these aspects be fully taken into account when assessing the CESI. This is especially true of the interconnections among these components.

Reasonable zoning policy

Ecological protection zone (I-1)
The increase in forest land in the region will help improve the level of ecosystem service supply, strengthen the implementation of the project of returning farmland to forest and forest protection, and use science and technology to prepare for early warning and emergency response. Plant suitable trees scientifically according to the terrain and slope, and build secondary forests and ecological public welfare forests.

Ecological construction zone (I-2)
The ecosystem supply in this area is not stable enough. In order to avoid excessive vegetation cover, which will lead to strong evapotranspiration and damage the water cycle[81], it is recommended to moderately return farmland to forest and reasonably manage vegetation. Repair damaged ecological areas and replenish ecological water to enhance the region's ability to resist natural risks.

Cultivated land management zone (II-1)
The soil has a high potential for loss and low water production capacity. It is recommended to scientifically plan land use and use conservation tillage. Develop water-saving industries to improve water resource utilization and reduce soil and water loss[51]. Optimize the agricultural environment, establish ecological buffer zones, protect biodiversity, promote green agricultural production, and reduce the use of chemical fertilizers and pesticides[22].

Urban construction zone (II-2)
To enhance ecological functions, it is necessary to strictly control urban sprawl, protect urban water bodies, and promote rainwater collection and utilization systems. At the same time, we will expand the urban green space, build an urban green network[82], promote green lifestyles, optimize water resource utilization efficiency, and improve urban ecological efficiency.

Limitations and prospects
This study has the following limitations: First, due to the strong humanistic attributes of cultural services (such as recreation and aesthetic value) and their indirect correlation with the policy of GFGP, they were not included in the ecosystem service analysis framework, making it difficult to fully reflect the overall status of ecosystem services. Secondly, at the methodological level, the Mann–Kendall trend test has high requirements for sample size, which may affect the accuracy of trend detection when data is insufficient. The bandwidth selection and kernel function parameterization of the MGWR model are subjective, which may lead to deviations in the characterization of spatial heterogeneity. It is sensitive to sample size and spatial autocorrelation and is prone to overfitting or underfitting problems. In addition, the overall accuracy of the 30-m CLCD used is 80%, and the land use types in the transition zone are vaguely defined, affecting the accuracy of ecosystem service assessment. At the same time, the study only focused on the township scale and failed to reveal the driving mechanism of ecosystem services at the grid or watershed scale, limiting the comprehensive understanding of multi-scale spatial heterogeneity. Future research needs to incorporate cultural service indicators and optimize parameter selection methods to reveal the dynamic changes and interaction mechanisms of ecosystem services at different spatial scales.

Conclusions
This study conducted a quantitative assessment of four key ESs in the Luo River Basin from 1999 to 2020 and used the Sen + MK trend test to identify the significance of long-term temporal change trends of ESs. The spatial clustering combination patterns of different ESs were analyzed by combining CESI and ES bundles, enriching the ESs evaluation framework. The OPGD and MGWR models were used to reveal the spatial response mechanism of the dominant driving factors and propose a zoning management strategy. The results show that:

(1)Ecosystem services showed significant differentiation characteristics, and the high-value areas were highly consistent with the distribution of forest land, indicating that the project of returning farmland to forest has a significant promoting effect on the improvement of ESs. WY, CS, and SR grew at an average annual rate of 4.71%, 0.05%, and 8.97% respectively, and their growth trend areas accounted for more than 90%. HQ, on the other hand, declined by an average of 0.31% per year, and its declining area reached 39.76%.

(2)The combination of CESI and ES bundles reveals the spatial reconstruction process of ESs and provides a new perspective for exploring the complex relationships among ESs. The comprehensive benefits of ecosystem services in the upstream forest area are better than those in the downstream. The integrated ecological bundle (B2) with a high synergistic supply of ESs in the upstream gradually transforms into the ecological protection bundle (B1) and the key synergistic bundle (B3), and the area of the downstream urban center bundle (B4) gradually expands.

(3)There is significant spatial heterogeneity in the driving mechanism, which shapes the spatial differentiation pattern of ESs. PRE, NDVI, and SLOPE are natural dominant factors of ESs and CESI (q > 0.55). PRE has a positive impact on WY and CESI, NDVI has a differentiated effect on CS, with a negative effect in the west and a positive effect in the east, and SLOPE has a significant positive impact on SR and HQ.

(4)Based on the characteristics of ecosystem services and driving response laws, a zoning management framework at the township scale was constructed. The research results provide a scientific basis for optimizing the implementation of the project of returning farmland to forest and coordinating ecological protection and regional development.

Data availability
All data generated or analysed during this study are included in this published article.

References
1. Costanza, R. et al. The value of the world's ecosystem services and natural capital. *Nature* **387**, 253–260. https://doi.org/10.1038/387253a0 (1997).
2. Li, D. L., Wu, S. Y., Liu, L. B., Liang, Z. & Li, S. C. Evaluating regional water security through a freshwater ecosystem service flow model: A case study in Beijing-Tianjian-Hebei region, China. *Ecol. Indic.* **81**, 159–170. https://doi.org/10.1016/j.ecolind.2017.05.034 (2017).
3. Li, Y., Ni, J., Yang, Q. & Li, R. Human impacts on soil erosion identified using land-use changes: A case study from the Loess Plateau, China. *Phys. Geogr.* **27**, 109–126. https://doi.org/10.2747/0272-3646.27.2.109 (2006).

4. Agency, X. N. *Outline of the Plan for Ecological Protection and High-Quality Development of the Yellow River Basin*, https://www.gov.cn/zhengce/2021-10/08/content_5641438.htm (2021)

5. Agency, X. N. *Opinions of the Central Committee of the Communist Party of China and the State Council on Accelerating the Advancement of the Construction of Ecological Civilization*, https://www.gov.cn/xinwen/2015-05/05/content_2857363.htm (2015).

6. Fu, B. et al. Assessing the soil erosion control service of ecosystems change in the Loess Plateau of China. *Ecol. Complex.* **8**, 284–293. https://doi.org/10.1016/j.ecocom.2011.07.003 (2011).

7. Schirpke, U. et al. Past and future impacts of land-use changes on ecosystem services in Austria. *J. Environ. Manage.* **345**, 118728. https://doi.org/10.1016/j.jenvman.2023.118728 (2023).

8. Stefanidis, S., Proutsos, N., Alexandridis, V. & Mallinis, G. Ecosystem services supply from Peri-Urban watersheds in Greece: soil conservation and water retention. *Land* **13**, 765. https://doi.org/10.3390/land13060765 (2024).

9. Hisano, M., Ghazoul, J., Chen, X. & Chen, H. Y. Functional diversity enhances dryland forest productivity under long-term climate change. *Sci. Adv.* **10**, eadn4152. https://doi.org/10.1126/sciadv.adn4152 (2024).

10. Bunel, R., Copard, Y., Massei, N. & Lecoq, N. Impact of vegetation cover on hydro-sedimentary fluxes in the marly badlands of the Southern Alps (Draix-Bléone Critical Zone Observatory, SE France). *Geomorphology* https://doi.org/10.1016/j.geomorph.2025.109726 (2025).

11. Bekri, E. S., Kokkoris, I. P., Skuras, D., Hein, L. & Dimopoulos, P. Ecosystem accounting for water resources at the catchment scale, a case study for the Peloponnisos, Greece. *Ecosyst. Serv.* **65**, 101586. https://doi.org/10.1016/j.ecoser.2023.101586 (2024).

12. Wang, J., Su, D., Wu, Q., Li, G. & Cao, Y. Study on eco-efficiency of cultivated land utilization based on the improvement of ecosystem services and emergy analysis. *Sci. Total Environ.* **882**, 163489. https://doi.org/10.1016/j.scitotenv.2023.163489 (2023).

13. Wang, S., Hu, M. M., Wang, Y. F. & Xia, B. C. Dynamics of ecosystem services in response to urbanization across temporal and spatial scales in a mega metropolitan area. *Sustain. Cities Soc.* **77**, 103561. https://doi.org/10.1016/j.scs.2021.103561 (2022).

14. An, Y., Zhao, W., Li, C. & Ferreira, C. S. S. Temporal changes on soil conservation services in large basins across the world. *Catena* https://doi.org/10.1016/j.catena.2021.105793 (2022).

15. Qu, J., Xu, Z., Dong, B., Wang, H. & Han, Y. J. Analyzing trade-offs, synergies, and driving factors of ecosystem services in Anhui Province using spatial analysis and XG-boost modeling. *Ecol. Indic.* **171**, 113098. https://doi.org/10.1016/j.ecolind.2025.113098 (2025).

16. Pan, H. H., Du, Z. Q., Wu, Z. T., Zhang, H. & Ma, K. M. Assessing the coupling coordination dynamics between land use intensity and ecosystem services in Shanxi's coalfields, China. *Ecol. Indic.* **158**, 111321. https://doi.org/10.1016/j.ecolind.2023.111321 (2024).

17. Wu, L. & Fan, F. Assessment of ecosystem services in new perspective: A comprehensive ecosystem service index (CESI) as a proxy to integrate multiple ecosystem services. *Ecol. Indic.* **138**, 108800. https://doi.org/10.1016/j.ecolind.2022.108800 (2022).

18. Huang, F. X. et al. Exploring the driving factors of trade-offs and synergies among ecological functional zones based on ecosystem service bundles. *Ecol. Indic.* **146**, 109827. https://doi.org/10.1016/j.ecolind.2022.109827 (2023).

19. Liao, Q., Li, T., Wang, Q. & Liu, D. Exploring the ecosystem services bundles and influencing drivers at different scales in southern Jiangxi, China. *Ecol. Indic.* **148**, 110089. https://doi.org/10.1016/j.ecolind.2023.110089 (2023).

20. Pellowe, K. E., Meacham, M., Peterson, G. D. & Lade, S. J. Global analysis of reef ecosystem services reveals synergies, trade-offs and bundles. *Ecosyst. Serv.* https://doi.org/10.1016/j.ecoser.2023.101545 (2023).

21. Reader, M. O., Eppinga, M. B., de Boer, H. J., Petchey, O. L. & Santos, M. J. Consistent ecosystem service bundles emerge across global mountain, island and delta systems. *Ecosyst. Serv.* **66**, 101593. https://doi.org/10.1016/j.ecoser.2023.101593 (2024).

22. Raudsepp-Hearne, C., Peterson, G. D. & Bennett, E. M. Ecosystem service bundles for analyzing tradeoffs in diverse landscapes. *Proc. Natl. Acad. Sci. USA* **107**, 5242–5247. https://doi.org/10.1073/pnas.0907284107 (2010).

23. Su, H. et al. Assessment of regional ecosystem service bundles coupling climate and land use changes. *Ecol. Indic.* **169**, 112844. https://doi.org/10.1016/j.ecolind.2024.112844 (2024).

24. Li, Y., Zhan, J., Liu, Y., Zhang, F. & Zhang, M. Response of ecosystem services to land use and cover change: A case study in Chengdu City. *Resour. Conserv. Recycl.* **132**, 291–300. https://doi.org/10.1016/j.resconrec.2017.03.009 (2018).

25. Li, B. J. et al. Spatio-temporal assessment of urbanization impacts on ecosystem services: Case study of Nanjing City, China. *Ecol. Indic.* **71**, 416–427. https://doi.org/10.1016/j.ecolind.2016.07.017 (2016).

26. Hao, R. F. et al. Impacts of changes in climate and landscape pattern on ecosystem services. *Sci. Total Environ.* **579**, 718–728. https://doi.org/10.1016/j.scitotenv.2016.11.036 (2017).

27. Li, J. Y. & Zhang, C. Exploring the relationship between key ecosystem services and socioecological drivers in alpine basins: A case of Issyk-Kul Basin in Central Asia. *Glob. Ecol. Conserv.* **29**, e01729. https://doi.org/10.1016/j.gecco.2021.e01729 (2021).

28. Peng, J. et al. Distinguishing the impacts of land use and climate change on ecosystem services in a karst landscape in China. *Ecosyst. Serv.* **46**, 101199. https://doi.org/10.1016/j.ecoser.2020.101199 (2020).

29. Sannigrahi, S. et al. Responses of ecosystem services to natural and anthropogenic forcings: A spatial regression based assessment in the world's largest mangrove ecosystem. *Sci. Total Environ.* **715**, 137004. https://doi.org/10.1016/j.scitotenv.2020.137004 (2020).

30. Liu, W. et al. Spatio-temporal variations of ecosystem services and their drivers in the Pearl River Delta, China. *J. Clean. Prod.* **337**, 130466. https://doi.org/10.1016/j.jclepro.2022.130466 (2022).

31. Li, G., Li, J., Zhao, C., Jiao, Y. & Yan, Q. Spatiotemporal dynamics of ecosystem services and their nonlinear influencing factors-A case study in the Qiantang River Basin. *China Environ. Sci.* **42**, 5941–5952. https://doi.org/10.19674/j.cnki.issn1000-6923.20220930.004 (2022).

32. Su, S. L., Li, D. L., Hu, Y. N., Xiao, R. & Zhang, Y. Spatially non-stationary response of ecosystem service value changes to urbanization in Shanghai, China. *Ecol. Indic.* **45**, 332–339. https://doi.org/10.1016/j.ecolind.2014.04.031 (2014).

33. He, L. et al. Exploring the interrelations and driving factors among typical ecosystem services in the Yangtze river economic Belt, China. *J. Environ. Manag.* https://doi.org/10.1016/j.jenvman.2023.119794 (2024).

34. Dong, Y. et al. Spatial-temporal evolution of vegetation NDVI in association with climatic, environmental and anthropogenic factors in the Loess Plateau, China during 2000–2015: quantitative analysis based on geographical detector model. *Remote Sens.* **13**, 4380. https://doi.org/10.3390/rs13214380 (2021).

35. Wang, X. et al. Identification of priority protected areas in Yellow River Basin and detection of key factors for its optimal management based on multi-scenario trade-off of ecosystem services. *Ecol. Eng.* **194**, 107037. https://doi.org/10.1016/j.ecoleng.2023.107037 (2023).

36. Guo, Y., Lu, X. & Ding, S. The classification of plant functional types based on the dominant herbaceous species in the riparian zone ecosystems in the Yiluo River. *Shengtai Xuebao/Acta Ecol. Sin.* **32**, 4434–4442. https://doi.org/10.5846/stxb201106270953 (2012).

37. Zhuang, D. & Liu, J. Study on the model of regional differentiationof land use degree in China. *J. Nat. Resour.* **12**, 105–111. https://doi.org/10.11849/zrzyxb.1997.02.002 (1997).

38. Assesment, M. E. Ecosystems and human well-being: Synthesis. *Phys. Teach* **34**, 534 (2005).

39. Ding, X. M. & Jian, S. Q. Synergies and trade-offs of ecosystem services affected by land use structures of small watershed in the Loess Plateau. *J. Environ. Manag.* https://doi.org/10.1016/j.jenvman.2023.119589 (2024).

40. Yang, D. et al. Estimation of water provision service for monsoon catchments of South China: Applicability of the InVEST model. *Landsc. Urban Plan.* **182**, 133–143. https://doi.org/10.1016/j.landurbplan.2018.10.011 (2019).

41. Yang, J., Xie, B. & Zhang, D. Spatio-temporal evolution of carbon stocks in the Yellow River Basin based on InVEST and CA-Markov models. *Chin. J. Eco-Agric.* **29**, 1018–1029. https://doi.org/10.13930/j.cnki.cjea.200746 (2021).

42. Xie, B. & Zhang, M. Spatio-temporal evolution and driving forces of habitat quality in Guizhou Province. *Sci. Rep.* **13**, 6908. https://doi.org/10.1038/s41598-023-35348-5 (2023).

43. Theil, H. *Henri Theil's Contributions to Economics and Econometrics: Econometric Theory and Methodology* 345–381 (Springer, 1992).

44. Nanditha, H. S., Reshmidevi, T. V., Simha, L. U. & Kunhikrishnan, P. Statistical analysis of rainfall and groundwater interaction in Bhadra catchment. *Environ. Dev. Sustain.* **26**, 16267–16287. https://doi.org/10.1007/s10668-023-03237-6 (2023).

45. Yuan, L. et al. The spatio-temporal variations of vegetation cover in the Yellow River Basin from 2000 to 2010. *Acta Ecol. Sin* **33**, 7798–7806. https://doi.org/10.5846/stxb201305281212 (2013).

46. Vesanto, J. & Alhoniemi, E. Clustering of the self-organizing map. *IEEE Trans. Neural Netw.* **11**, 586–600. https://doi.org/10.1109/72.846731 (2000).

47. Xia, H., Yuan, S. & Prishchepov, A. V. Spatial-temporal heterogeneity of ecosystem service interactions and their social-ecological drivers: Implications for spatial planning and management. *Resour. Conserv. Recycl.* **189**, 106767. https://doi.org/10.1016/j.resconrec.2022.106767 (2023).

48. Wang, J. & Xu, C. D. Geodetector: Principle and prospective. *Acta Geogr. Sin.* **72**, 116–134. https://doi.org/10.11821/dlxb201701010 (2017).

49. Song, Y., Wang, J., Ge, Y. & Xu, C. An optimal parameters-based geographical detector model enhances geographic characteristics of explanatory variables for spatial heterogeneity analysis: Cases with different types of spatial data. *GIScience Remote Sens.* **57**, 593–610. https://doi.org/10.1080/15481603.2020.1760434 (2020).

50. Huang, Z., Li, S., Peng, Y. & Gao, F. Spatial non-stationary of influencing factors of China's county economic development base on a multiscale geographically weighted regression model. *ISPRS Int. J. Geo Inf.* **12**, 109. https://doi.org/10.3390/ijgi12030109 (2023).

51. Chen, Y. et al. Identifying the spatial relationships and drivers of ecosystem service supply–demand matching: A case of Yiluo River Basin. *Ecol. Ind.* **163**, 112122. https://doi.org/10.1016/j.ecolind.2024.112122 (2024).

52. Li, L. et al. Spatiotemporal evolution and prediction of ecosystem carbon storage in the Yiluo River Basin Based on the PLUS-InVEST model. *Forests* **14**, 2442. https://doi.org/10.3390/f14122442 (2023).

53. Chen, W. X., Chi, G. Q. & Li, J. F. Ecosystem services and their driving forces in the middle reaches of the Yangtze River Urban Agglomerations, China. *Int. J. Environ. Res. Public Health* **17**, 3717. https://doi.org/10.3390/ijerph17103717 (2020).

54. Wang, S. & Noland, R. B. Variation in ride-hailing trips in Chengdu, China. *Transp. Res. Part D* **90**, 102596. https://doi.org/10.1016/j.trd.2020.102596 (2021).

55. Brunsdon, C., Fotheringham, A. S. & Charlton, M. E. Geographically weighted regression: a method for exploring spatial nonstationarity. *Geogr. Anal.* **28**, 281–298. https://doi.org/10.1111/j.1538-4632.1996.tb00936.x (1996).

56. Fotheringham, A. S., Yang, W. & Kang, W. Multiscale geographically weighted regression (MGWR). *Ann. Am. Assoc. Geogr.* **107**, 1247–1265. https://doi.org/10.1080/24694452.2017.1352480 (2017).

57. Oshan, T. M., Li, Z., Kang, W., Wolf, L. J. & Fotheringham, A. S. mgwr: A Python implementation of multiscale geographically weighted regression for investigating process spatial heterogeneity and scale. *ISPRS Int. J. Geo Inf.* **8**, 269. https://doi.org/10.3390/ijgi8060269 (2019).

58. Hu, Y., Zhang, S., Shi, Y. & Guo, L. Quantifying the impact of the Grain-for-Green Program on ecosystem service scarcity value in Qinghai, China. *Sci. Rep.* **13**, 2927. https://doi.org/10.1038/s41598-023-29937-7 (2023).

59. Qiao, X., Zhang, J., Liu, L., Zhang, J. & Zhao, T. Spatiotemporal changes in vegetation cover during the growing season and its implications for Chinese grain for green program in the Luo River Basin. *Forests* **15**, 1649. https://doi.org/10.3390/f15091649 (2024).

60. Hayes, A. F. & Cai, L. Using heteroskedasticity-consistent standard error estimators in OLS regression: An introduction and software implementation. *Behav. Res. Methods* **39**, 709–722. https://doi.org/10.3758/BF03192961 (2007).

61. Huang, Y. T. & Wu, J. Y. Spatial and temporal driving mechanisms of ecosystem service trade-off/synergy in national key urban agglomerations: A case study of the Yangtze River Delta urban agglomeration in China. *Ecol. Ind.* **154**, 110800. https://doi.org/10.1016/j.ecolind.2023.110800 (2023).

62. Zhang, R. et al. Spatial-temporal pattern and driving factors of flash flood disasters in Jiangxi province analyzed by optimal parameters-based geographical detector. *Geogr. Geo-Inform. Sci* **37**, 72–80. https://doi.org/10.3969/j.issn.1672-0504.2021.04.011 (2021).

63. Jia, Y. F. & Wang, G. Q. Assessment of water conservation capacity of Yiluo River Basin Based on the InVEST Model. *J. Soil Water Conserv.* **37**, 101–108. https://doi.org/10.13870/j.cnki.stbcxb.2023.03.014 (2023).

64. Nouri, A. et al. Conservation agriculture increases the soil resilience and cotton yield stability in climate extremes of the southeast US. *Commun. Earth Environ.* **2**, 155. https://doi.org/10.1038/s43247-021-00223-6 (2021).

65. Wang, S., Zhang, Y., Wei, H. & Zhang, H. The NPP change and the vegetation carbon fixation/oxygen release values in Shaanxi-Gansu-Ningxia Region of China. *J. Desert Res.* **35**, 1421–1428. https://doi.org/10.7522/j.issn.1000-694X.2014.00196 (2015).

66. Liao, Z. et al. Growing biomass carbon stock in China driven by expansion and conservation of woody areas. *Nat. Geosci.* https://doi.org/10.1038/s41561-024-01569-0 (2024).

67. Efthimiou, N. & Psomiadis, E. The significance of land cover delineation on soil erosion assessment. *Environ. Manage.* **62**, 383–402. https://doi.org/10.1007/s00267-018-1044-3 (2018).

68. Panagos, P. et al. Estimating the soil erosion cover-management factor at the European scale. *Land Use Policy* **48**, 38–50. https://doi.org/10.1016/j.landusepol.2015.05.021 (2015).

69. Gnann, S. et al. The influence of topography on the global terrestrial water cycle. *Rev. Geophys.* **63**, e2023RG000810. https://doi.org/10.1029/2023RG000810 (2025).

70. Feng, X. M. et al. Revegetation in China's Loess Plateau is approaching sustainable water resource limits. *Nat. Clim. Chang.* **6**, 1019–1022. https://doi.org/10.1038/nclimate3092 (2016).

71. Xue, C. et al. Modeling the spatially heterogeneous relationships between tradeoffs and synergies among ecosystem services and potential drivers considering geographic scale in Bairin Left Banner, China. *Sci. Total Environ.* **855**, 158834. https://doi.org/10.1016/j.scitotenv.2022.158834 (2023).

72. Alcamo, J. et al. Changes in ecosystem services and their drivers across the scenarios. *Ecosyst. Hum. Well-Being* **2**, 297–373 (2005).

73. Li, C., Qiao, W., Gao, B. & Chen, Y. Unveiling spatial heterogeneity of ecosystem services and their drivers in varied landform types: Insights from the Sichuan-Yunnan ecological barrier area. *J. Clean. Prod.* **442**, 141158. https://doi.org/10.1016/j.jclepro.2024.141158 (2024).

74. Jia, Z. X. et al. Exploring the spatial heterogeneity of ecosystem services and influencing factors on the Qinghai Tibet Plateau. *Ecol. Ind.* **154**, 110521. https://doi.org/10.1016/j.ecolind.2023.110521 (2023).

75. Song, J., Aishan, T. & Ma, X. Coupled water-habitat-carbon nexus and driving mechanisms in the Tarim River Basin: A multi-scenario simulation perspective. *Ecol. Ind.* **167**, 112649. https://doi.org/10.1016/j.ecolind.2024.112649 (2024).

76. Li, Y. & Luo, H. Trade-off/synergistic changes in ecosystem services and geographical detection of its driving factors in typical karst areas in southern China. *Ecol. Ind.* **154**, 110811. https://doi.org/10.1016/j.ecolind.2023.110811 (2023).

77. Fang, L. L. et al. Identifying the impacts of natural and human factors on ecosystem service in the Yangtze and Yellow River Basins. *J. Clean. Prod.* **314**, 127995. https://doi.org/10.1016/j.jclepro.2021.127995 (2021).

78. Zhang, Q. et al. Response of erosion reduction effect of typical soil and water conservation measures in cropland to rainfall and slope gradient changes and their applicable range in the Chinese Mollisols Region, Northeast China. *Int. Soil Water Conserv. Res.* **11**, 251–262. https://doi.org/10.1016/j.iswcr.2022.10.005 (2023).

79. Du Viet, Q. V. et al. Deep learning to assess the effects of land use/land cover and climate change on landslide susceptibility in the Tra Khuc river basin of Vietnam. *Geocarto Int.* https://doi.org/10.1080/10106049.2023.2172218 (2023).
80. Sun, X. Y., Jiang, Z., Liu, F. & Zhang, D. Z. Monitoring spatio-temporal dynamics of habitat quality in Nansihu Lake basin, eastern China, from 1980 to 2015. *Ecol. Ind.* **102**, 716–723. https://doi.org/10.1016/j.ecolind.2019.03.041 (2019).
81. Li, Y. G. et al. Quantitative assessment for the spatiotemporal changes of ecosystem services, tradeoff-synergy relationships and drivers in the semi-arid regions of China. *Remote Sens.* **14**, 239. https://doi.org/10.3390/rs14010239 (2022).
82. Li, Q. et al. Spatial heterogeneity of ecosystem service bundles and the driving factors in the Beijing-Tianjin-Hebei region. *J. Clean. Prod.* **479**, 144006. https://doi.org/10.1016/j.jclepro.2024.144006 (2024).

Acknowledgements

Author contributions

Conceptualization, J.Z. (Jing Zhang) and X.Q.; methodology, J.Z. (Jinchan Zheng); software, Y.Y.; validation, L.L. and J.Z. (Jinchan Zheng); formal analysis, Y.C. and Y.D.; investigation, J.Z. (Jing Zhang); resources, X.Q.; data curation, Y.Y.; writing—original draft preparation, J.Z. (Jing Zhang); writing—review and editing, X.Q.; visualization, L.L.; funding acquisition, X.Q. All authors have read and agreed to the published version of the manuscript. All authors have read and agreed to the published version of the manuscript.

Funding

Competing interests

The authors declare no competing interests.

Additional information